S8

Gravity Waves, Tides, and Coastal Oceanography: Supplementary Materials

This web-based content continues the topics of Chapter 8, covering several different aspects of coastal oceanography (river runoff, estuaries, and coral reefs in Sections S8.7, S8.8, and S8.9), followed by an extended discussion of adjacent seas (Section S8.10), including the Mediterranean, Black, Baltic, and North Seas from the Atlantic; the Bering, Okhotsk, Japan (East), Yellow, East China, South China Seas, and Gulf of California from the Pacific Ocean; and the Red Sea and Persian Gulf from the Indian Ocean.

Figure numbering in this portion of Chapter 8 continues from the last figure of the print text but with "S" denoting online material, thus starting with Figure S8.16.

S8.7. WATER PROPERTIES IN COASTAL REGIONS: RIVER RUNOFF

River runoff affects coastal regions. It reduces the salinity of the surface layer and even of the deeper water if there is sufficient vertical mixing. It often carries a large amount of suspended sediment, as seen for the Mississippi River outflow and the outflows from the Himalayas into the Bay of Bengal, including the Ganges River (Figure S8.16). Generally, river runoff has a pronounced seasonal variation, resulting in much larger seasonal fluctuations of salinity in coastal waters than in the open ocean. In a coastal region where precipitation occurs chiefly as rain, the seasonal salinity variation will closely follow the local precipitation pattern. In regions where rivers are fed by meltwater from snowfields or glaciers, the river runoff increases in the summer to many times the winter rate and causes a corresponding decrease of salinity that lags the snowfall by several months.

Fresh river water flowing out over saltier open ocean water creates a strong halocline, with high vertical stability. This can inhibit mixing with water below the halocline. In the warm seasons, this can result in higher temperatures in the surface layer. In winter in high northern latitudes, the halocline permits the surface layer to cool to below the temperature of the water beneath the halocline, producing a temperature inversion. Ice thus tends to form first in coastal waters, as "fast ice" (Section 3.9.1; the shallowness of the coastal region also contributes). In regions of multiyear ice such as the Arctic, the new coastal ice spreads seaward until it contacts the first-year ice spreading shoreward from the multiyear pack ice.

Since river water frequently carries suspended sediment (Figure S8.16), coastal waters
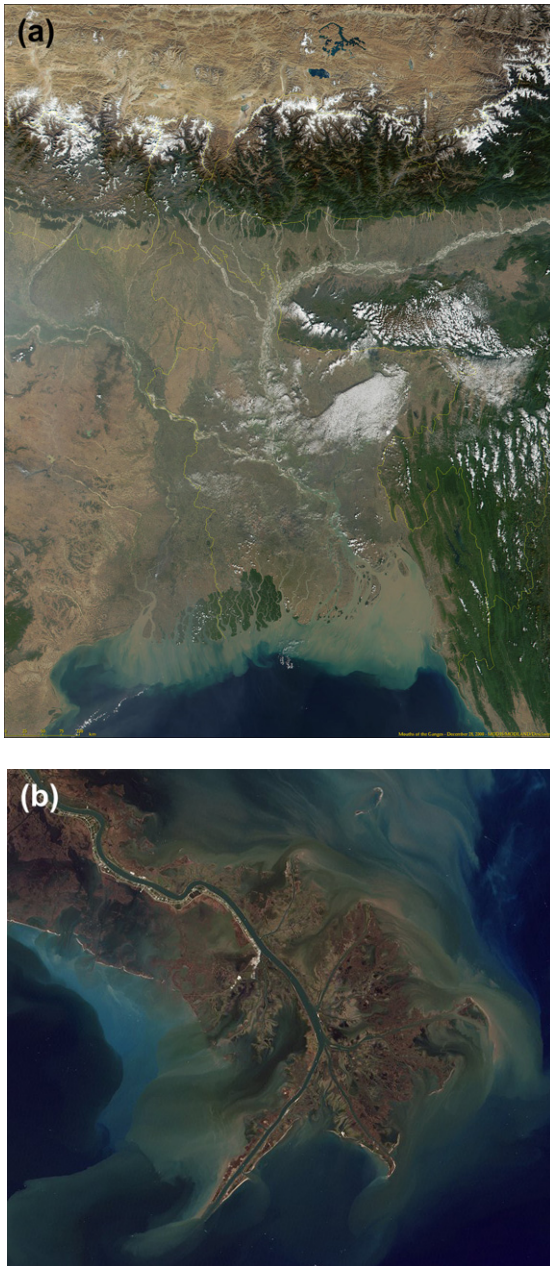
FIGURE S8.16 (a) Sediments in the Ganges River plume in the northern Bay of Bengal. The Himalayas are the line of snow-covered mountains across the top of the image; the whites in the center right are clouds. (b) Mississippi River estuary. Images from the Moderate Resolution Imaging Spectroradiometer (MODIS). *Source: From NASA Goddard Earth Sciences, (2007c, 2008).*

often have low optical transparency (Section 3.8.1). Sometimes this sediment is carried in the surface low-salinity layer for some distance while the deeper, more saline water remains clear. The deposition of this sediment causes shoaling and consequent hazards to navigation. Frequently the location of the deposition is influenced by the salinity distribution because increases in salinity can cause flocculation of the sediment and rapid settling.

The effect of runoff, especially from large rivers, can often be traced a long way from the coast, both by reduced salinity and by the sediment in the water. Some examples of major influences on the open ocean include the Amazon and Congo Rivers in the tropical Atlantic, in the northeast Pacific from the many rivers flowing off the North American continent, and in the Bay of Bengal from the large rivers whose runoff is strongly influenced by the monsoon. Low salinity from these river sources can be seen even in the global surface salinity map (Figure 4.16). The net freshwater input from these sources is an important part of the ocean's freshwater budget as apparent in the list of outflows of the major rivers of the world in order of volume transport in Dai and Trenberth (2002). Runoff is comparable to open ocean precipitation and evaporation because it deposits net precipitation over land into the ocean.

The result of the sediment deposition from runoff into the Bay of Bengal is apparent even in open ocean bottom topography, as a smooth sediment fan spreading down to 5000 m depth, across the equator in the Indian Ocean, evident in the bathymetry in Figure 4.13 (Curray, Emmel, & Moore, 2003).

S8.8. ESTUARIES

An estuary, in the strictest definition, is formed at the mouth of a river, where the river meets the sea (Dyer, 1997). Cameron and Pritch-ard (1963) defined an *estuary* as "a semi-enclosed

coastal body of water having a free connection to the open sea and within which the sea-water is measurably diluted with fresh water deriving from land drainage." They restrict the definition to coastal features and exclude large bodies of water such as the Baltic Sea. The river water, which enters the estuary, mixes to some extent with the salt water therein and eventually flows out to the open sea in the upper layer. The mixing processes are mainly due to tides and the wind. A corresponding inflow of seawater takes place below the upper layer. The inflow and outflow are dynamically associated so that while an increase in river flow tends to reduce the salinity of the estuary water, it also causes an increased inflow of seawater, which tends to increase the salinity. Thus an approximate steady state prevails.

The defining characteristic of estuarine circulation is that inflow is denser than outflow, which is diluted relative to the inflow. Sometimes this concept is applied heuristically to much larger bodies of water, such as the Black Sea, or even the Indian and Pacific Oceans, but the study of estuarine circulation is defined to be within the confined coastal regions.

Extended descriptions of estuaries and estuarine circulation can be found in the texts by Dyer (1997), Officer (1976), and Hardisty (2007). Compilations of papers on specific estuaries or types of estuaries have appeared over the years. Beardsley and Boicourt (1981) summarized the Middle Atlantic Bight and Gulf of Maine; Farmer and Freeland (1983) reviewed the physical oceanography of fjord estuaries; papers in Neilson, Kuo, & Brubaker (1989) summarized then-contemporary ideas about estuaries; and the Estuarine and Coastal Science Association periodically produces compilations of papers.

S8.8.1. Types of Estuaries

There are many types of estuaries and many types of flow in estuaries. A classification system is useful as an introduction, but inevitably results in oversimplification (Pritchard, 1989). Estuaries are classified in terms of both their shape and their stratification. They can also be classified in terms of tidal and wind forcing. The inland end of an estuary is called the *head* and the seaward end the *mouth*. "Positive" estuaries have a river or rivers emptying into them, usually at the head.

In terms of geology, three specific types of estuary are recognized: the coastal plain (drowned river valleys), the deep basin (e.g., fjords), and the bar-built estuary; there are also types that do not fit in these categories (Dyer, 1997; Pritchard, 1989). The first is the result of land subsidence or a rise of sea level that floods a river valley; North American examples are the St. Lawrence River valley and Chesapeake Bay. Typical examples of the deep basin are the fjords of Norway, Greenland, Canada, South America, and New Zealand. Most of these have a sill or region toward the seaward end, which is shallower than both the main basin of the fjord and the sea outside, so it restricts the exchange of deep water. The third type is the narrow channel between the shore and a bar, which has built up close to shore through sedimentation or wave action.

In terms of stratification and salinity structure, estuaries have been classified based on the distribution of water properties as (a) vertically mixed, (b) slightly stratified, (c) highly stratified, and (d) salt wedge estuaries (Figure S8.17; Dyer, 1997; Pritchard, 1989). The stratification is due to salinity, because density in estuaries is determined mainly by salinity rather than by temperature. The classification system is not rigid. In the left-hand column of Figure S8.17, the salinity distributions are shown as vertical profiles at each of four stations between the head and the mouth of the estuary (see schematic plan view at the top). The right-hand column shows simplified longitudinal sections of salinity from head to mouth for the full depth of the estuary. In most estuaries, unlike the schematics in Figure S8.17, the bottom depth is shallowest at the head.
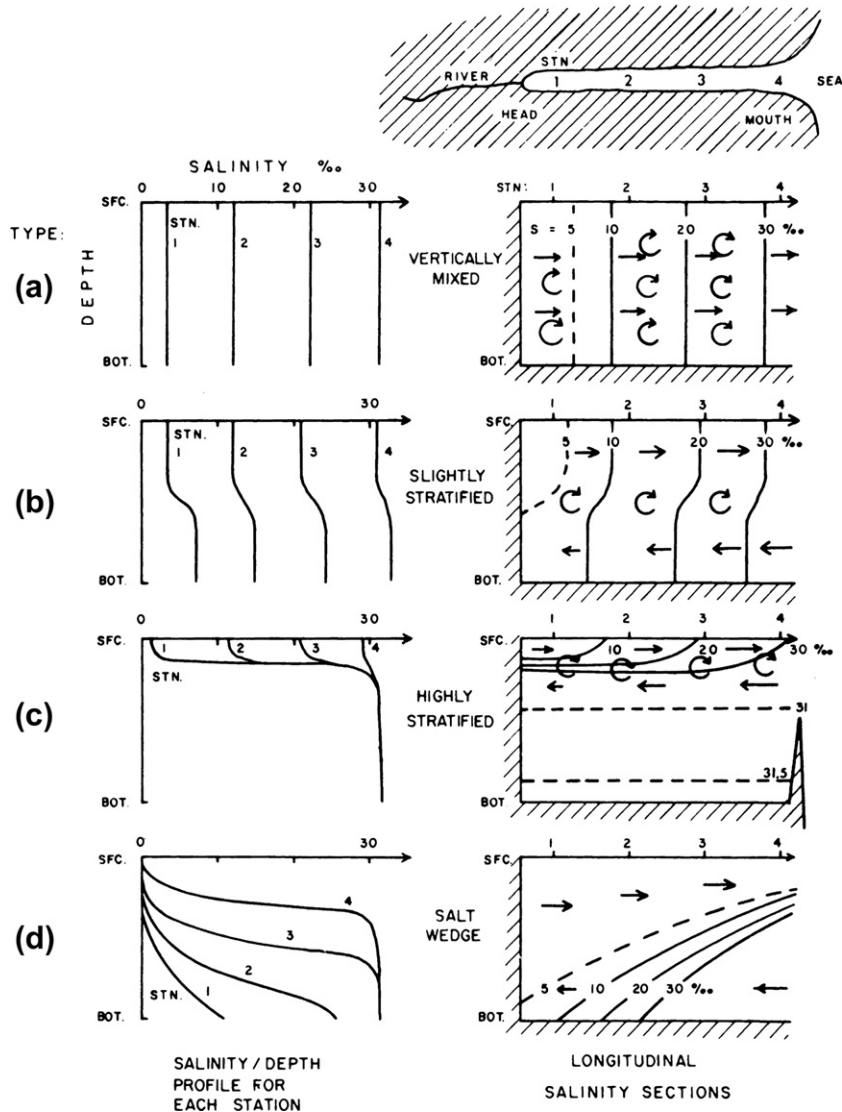
FIGURE S8.17 Typical salinity/depth profiles (left) and longitudinal salinity sections (right) in different types of estuaries: (a) vertically mixed, (b) slightly stratified, (c) highly stratified, and (d) salt wedge.

The *vertically mixed estuary* (Figure S8.17a) is generally shallow and the water is mixed vertically making it homogeneous from the surface to the bottom at any particular place along the estuary. The salinity increases with distance along the estuary from head to mouth. The river water in this type of estuary flows toward the mouth while the salt may be considered to progress from the sea toward the head by eddy diffusion at all depths. In the right-hand figure, the vertical isohalines indicate the homogeneity of the water at each location while the straight

arrows indicate that the direction of net flow of the water is seaward at all depths. (The circular arrows symbolize the mixing taking place at all depths.) The Severn River in England is an example of a vertically mixed estuary.

In the *slightly stratified estuary* (Figure S8.17b), which is usually also shallow, the salinity increases from head to mouth at all depths. The water is essentially in two layers with the upper layer a little less saline than the deeper one at each position along the estuary, with a mixing layer between them (symbolized by the circular arrows in Figure S8.17b). In this type of estuary there is a net seaward (outward) flow in the upper layer and a net inward flow in the deeper layer as shown by the straight arrows in the vertical salinity section. In addition to these flows at both levels there is the vertical mixing of both fresh and salt water giving rise to the longitudinal variation of salinity in both layers. The James River in Chesapeake Bay is an example of this type of estuary.

In the *highly stratified estuary* (Figure S8.17c), of which fjords are typical, the upper layer increases in salinity from near zero in the river at the head to a value close to that of the outside sea at the mouth. The deep water, however, is of almost uniform salinity from head to mouth. Again there is a net outflow in the upper layer and inflow in the deeper water as shown by the straight arrows in the salinity section. In these estuaries there is a very strong halocline between the upper water and the deep water, particularly at the head where vertical salinity gradients of 10 to 20 psu per meter may occur in summer during the period of greatest river runoff. There is vertical mixing, but this results predominantly in an upward movement of salt water from below into the upper layer, with little downward movement of fresh water. One explanation for this almost unidirectional mixing is that internal waves are generated by the velocity shear between the upper low salinity layer and the deeper more saline water, and that the tops of these waves break and throw off a "spray" of saline water into the upper layer into which it mixes. There is much less breaking at the bottom of the internal waves and therefore no spray of fresh water downward into the saline water.

For the *salt wedge estuary* (Fig S8.17d), the longitudinal section indicates the reason for its name. The saline water intrudes from the sea as a wedge below the river water. This situation is typical of rivers of large volume transport such as the Fraser or Mississippi Rivers (Figure S8.16b). It should be noted that the section in Figure S8.17 is exaggerated in the vertical direction; the salt wedge really has a much smaller angle than shown, with almost horizontal isohalines.

The salt wedge estuary has features in common with the stratified estuaries. There is a horizontal gradient of salinity at the bottom as in a slightly stratified estuary and a pronounced vertical salinity gradient as in a highly stratified estuary. The distinction is in the lack of saline water at the surface until it reaches the sea at the mouth of the estuary, because of the large river flow. In this type of estuary the salt wedge migrates up and down the estuary as the tide floods and ebbs, sometimes by several kilometers.

In terms of mixing, Stommel (reported by Pritchard, 1989) suggested that estuaries be classified in terms of tidal and wind forcing, which are the main modes of mixing in estuaries. The tides that are important in estuaries are almost always co-oscillation tides (Section 8.6.2). This classification has evolved to consider the tidal range and effect of friction on tides in the estuary (Dyer, 1997). Both the winds and tides have temporal and spatial variations. The stratification in an estuary can therefore vary significantly with time as well as location in the estuary.

S8.8.2. Estuarine Circulation

In an estuary, the flow is out to the ocean in the upper layer and into the estuary in the bottom layer. In stratified estuaries, the depth

of the halocline (thickness of the upper, low salinity layer) remains substantially constant from head to mouth of an estuary for a given river runoff. If the estuary width does not change much, then the depth remains constant, which means that the cross-sectional area of the upper layer outflow remains the same while its volume transport increases because of the entrainment of salt water from below. Consequently, the speed of the outflowing surface layer markedly increases along the estuary from head to mouth. The increase in volume and speed can be considerable, with the outflow at the mouth as much as 10 to 30 times the volume flow of the river. In his classical study of Alberni Inlet — a typical, highly stratified, fjord-type estuary in British Columbia — Tully (1949) demonstrated the above features. He also showed that the depth of the upper layer decreased as the river runoff increased up to a critical value and thereafter increased as runoff increased.

Estuarine circulation depends on several factors: the sill depth, river runoff rate, and the character of the outside water density distribution. Tides and mixing also impact the circulation. If the sill is so shallow that it penetrates into the low-salinity, out-flowing upper layer, the full estuarine circulation cannot develop and the subsurface inflow of saline water does not occur regularly. As a result, the deep water is not exchanged regularly and tends to become stagnant. This situation occurs in some of the smaller Norwegian fjords, but is by no means typical of deep basin estuaries. Most of the fjords in Norway, as well as on the west coasts of North and South America and New Zealand, have sills that are deeper than the upper layer. Therefore the estuarine circulation is developed sufficiently to affect continual renewal of the deep water and stagnation does not occur (Pickard, 1961; Pickard & Stanton, 1980). The rate of renewal is proportional to the circulation, which is proportional to the river runoff. Fjord estuaries with small river runoff show more

evidence of limited circulation in the form of low oxygen values than those with large runoff. The depth of the sill has little effect as long as it is greater than the depth of the low-salinity, out-flowing upper layer.

The other major factor influencing the exchange of the deep basin water is seasonal variation in the density structure of the outside seawater. Although the downward mixing of fresh water in an estuary is small, it does occur to some extent. Therefore the salinity, and hence the density of the basin water, tends to decrease slowly. If a change then occurs in the outside water such that the density outside becomes greater than that inside at similar levels above the sill depth, then there will be an inflow of water from the sea. The inflowing water is likely to sink, although not necessarily to the bottom, in the estuary basin and displace upward and outward some of the previously resident water. In this way the basin water becomes refreshed. In deep-sill estuaries this refreshment may occur annually, but in shallow-sill estuaries it may occur only at intervals of many years; the disturbance to the biological regime may be cataclysmic on these occasions (by displacing upward into the biotic zone the low-oxygen water from the bottom). This type of basin-water replacement has been well documented for some Norwegian fjords (with very shallow sills), but it should not be considered characteristic of all fjord estuaries.

The previous remarks only briefly describe some of the salient characteristics of stratified estuaries; the property distributions in Figure S8.17 are smoothed and schematic. Real distributions show fine and mesoscale structure and detailed features, some general and some local. In particular, because the density structure is determined largely by the salinity distribution, temperature maxima and minima are quite common in the water column. Mixing between fresh and salt water is largely governed by tidal movements and the effects of internal waves. The circulation that was just reviewed for

stratified estuaries is greatly modulated by the strong tidal currents in the estuaries. This brief description also neglects the horizontal variability and horizontal circulation in estuaries.

Estuarine characteristics and processes are observed in ocean areas as well as near the coast. In the northeast Pacific and in the Bay of Bengal, where there is considerable river runoff, the density of the upper layer is controlled by the salinity rather than by temperature as is usually the case in the open ocean. The upper, low-salinity layer of perhaps 100 m depth in the northeast Pacific is much less dense than the deeper, more saline water and the stability in the halocline between them inhibits mixing. Consequently, the summer input of heat is trapped in the surface layer and a marked seasonal thermocline develops as shown in Figure 4.8.

S8.8.3. Flushing Time of Estuaries

The time that it takes to replace the freshwater within an estuary through river discharge is called the *flushing time*. This is important for water quality within estuaries. The flushing time has significant temporal variation, especially since river flows have strong variability. Following Dyer (1997), the flushing time is the freshwater volume (V_F in units of m^3) divided by the river discharge (R, in units of m^3/sec). Both the freshwater volume and the river discharge can be time dependent. Using observations of the average salinity $<S>$ within the estuary compared with the seawater salinity S_o outside the estuary, the freshwater fraction can be estimated as $F = (S_o - <S>)/S_o$. The freshwater volume is the total volume, V, multiplied by the freshwater fraction. The flushing time is then

$$t_F = V_F/R = FV/R. \qquad (S8.10)$$

Flushing times range from several days to a year. Dyer lists flushing times for several estuaries: Narragansett Bay, Massachusetts − 12 to 40 days depending on river flow; Mersey − 5.3 days; Bay of Fundy − 76 days; and the Severn Estuary − 100 to 300 days depending on river flow.

Observing the salinity at all locations in the estuary at all times is unrealistic, so various approximate methods are used to determine the flushing time. Dyer (1997) is a good source for these different methods.

S8.9. CORAL REEFS

The physical oceanography of coral reefs was of particular interest to George Pickard, the original author of this text. He published several papers and a book on the Great Barrier Reef in 1977 (Pickard, Donguy, Henin, & Rougerie, 1977). Therefore we retain this section of Chapter 8, but it has not been updated. Many papers and some books have been published on the physical oceanography of coral reefs since the previous edition, and Wolanski (2001) and Monismith (2007) are suggested as starting points.

Prior to about 1970, most physical oceanography in coral reef areas had been carried out as ancillary to biological or chemical studies. Studies of the dynamics started in the late 1970s with most studies carried out in the Great Barrier Reef of Australia. Through the 1980s, of the 200 publications on the physical oceanography of coral reef regions, 70% refer to the Great Barrier Reef and only about 30% to other reef areas. Because of observed degradation of coral reefs worldwide, coral reef research expanded greatly in the 1990s, with numerous reefs now the focus of careful, ongoing studies — many with physical oceanographic components.

S8.9.1. Topography of Coral Reefs

Coral reefs are features of many coastal regions between the tropics, along the continental shelves, around islands, and also on the tops of shoals and seamounts in the open ocean

with little or no emergent land in their vicinity, such as atolls. Reefs act as complex barriers to flow in their neighborhood. Living coral cannot withstand exposure above water so it only occurs below low-tide level; it also requires light for growth so it generally cannot survive below about 50 m depth.

Along a land boundary, two types of reef are recognized: (1) the *fringing reef*, which extends out from the shore and (2) the *barrier reef*, which is located away from the shore with a relatively reef-free region (lagoon) between it and the shore. Despite its name, a barrier reef is rarely continuous for very long distances; instead it consists of a series of reefs with gaps between them. Water exchange with the ocean can take place through the gaps as well as over the reefs. In some cases the outer reefs may be long (parallel to the coast) and narrow; in others, the "barrier" may consist of a number of individual reefs dotted over a relatively wide band (50 km or more) parallel to the shore, with irregular passages between them connecting the lagoon with the open ocean outside. Open ocean reefs, based on shoals or seamounts, usually extend around the shoals; the "lagoon" is the body of shallow water within the reef perimeter, which usually has gaps that permit some direct exchange with the ocean. *Atolls* are reefs where sufficient material has collected on parts of the reef to raise the level a few meters above sea level and on which shrubs and trees may grow.

S8.9.2. Water Properties in Coral Reefs

Extensive and long-term measurements of water properties have been made in the Great Barrier Reef; in the southwest lagoon of New Caledonia; and in the Hawaiian, Floridian, and Caribbean reefs. The annual variation of water temperature is generally approximately sinusoidal with the maximum in the local summer and closely correlated with the air temperature. The annual range of temperature variation decreases toward the equator.

Salinity variations are less regular than those of temperature. Near land, decreases occur due to local precipitation and river runoff associated with monsoons, whereas for atolls only precipitation is effective. Increases of salinity are due to evaporation. An increase from an oceanic value of 35.7 psu near the pass into Canton Island lagoon to 39.5 psu at the back of the lagoon approximately 15 km away was recorded, but this is probably an extreme example.

Water depths in lagoons and around reefs are generally small, less than 50−100 m, and the water is usually unstratified, for example, well-mixed vertically due to turbulence from wind-wave effects and the rough character of the bottom over the reefs. Some stratification in the upper 10−20 m occurs near river mouths during periods of heavy runoff, but even then the variations in the vertical are generally less than $1°C$ in temperature and 1psu in salinity. Along the Great Barrier Reef, intrusions of cooler, more saline water can be evident near the bottom of passes through the outer reefs with $\Delta t = -5°C$ and $\Delta S = +1$ psu relative to the upper layer reef-area waters. In the very shallow water over fringing reefs, diel (day-night) variations of as much as 10 to $12°C$ have been observed and attributed to solar heating during the day and radiant cooling at night. It is probable that the relatively reef-free lagoon between the shore and off-lying barrier reefs occurs because coral is intolerant both of the fresh water and silt carried in by rivers.

S8.9.3. Currents in Coral Reefs

To describe the currents we divide them into three classes: drift or long-period (periods of weeks or more), weather band (periods of days), and tidal (periods of hours). Drift currents are generated by steady wind stress (e.g., the trade winds) or long-shore pressure gradients. The oceanic equatorial currents generated by the trade winds cause flow over the mid-ocean reefs, such as at Bikini. In the central Great

Barrier Reef, a 25-year time series of current measurements showed equatorward currents of 20 cm/sec during the south-east Trade Wind season, while at other times there was a poleward current of about 30 cm/sec attributable to the downward slope to the south associated with the southward flow of the East Australian Current outside the Great Barrier Reef.

Weather band currents associated with continental shelf waves have also been documented for the central and southern Great Barrier Reef. They are a consequence of fluctuations of wind stress as weather systems move eastward with their centers over the southern part of Australia. The weather systems have periods of 10 to 20 days and speeds of some 500 km/day (equatorward). As the resulting ocean currents have a vertical range of only 10 to 30 cm (near the shore and diminishing to zero outside the reef), they are not evident to the eye and can only be identified by analysis of tide or current records. Water particle speeds are approximately 20–40 cm/sec or 17–35 km/day. This can result in long-shore displacements of water of 100 to 200 km that can be very significant in transporting pollutants or plankton over such distances in the reef area.

Tidal-flows through reef passes of approximately 200 cm/sec are common; speeds as high as 370 cm/sec (13 km/h) at Aldabra Atoll have been recorded. It should be noted that although such tidal speeds through passes can be large, the inflowing water then spreads out in the lagoon and the distance of penetration of ocean water during the flood (which only lasts about 6 hours) may be only a few kilometers. This is small compared to the diameter of many atoll lagoons and therefore tidal flows may only have a limited effect on water exchange and flushing. Also, it has been observed that there is often little mixing between the intruding ocean water and the resident lagoon water.

The term "reef flat" refers to extensive areas of coral of relatively uniform height; the water depths over them are generally only a few meters. Flow over them may be due to drift currents, shelf waves, and tidal currents as well as to the local wind stress. Note that as the water in these areas is very shallow, bottom friction is more important than Coriolis force so the wind-driven flow is downwind, not to the left or right of the wind direction as in deeper water (see Section 7.5.3). Tidal currents over the reef flats may have speeds of 100 cm/sec or more. These flows (over the surrounding reef) will not necessarily go into a lagoon during the flood or out during the ebb. For instance, in the Great Barrier Reef, the tide wave approaches from the northeast so that the tidal flow in the area during the flood is to the southwest and can be over a surrounding reef into its lagoon on the northeast side but out of the lagoon on the southwest side at the same time. Wave-overtopping also contributes to the water in a reef lagoon. This occurs when ocean waves or swells break on the outside of a reef generating a slope across the reef, which causes flow across it. This component can contribute as much transport across a reef as the other mechanisms combined.

S8.9.4. Circulation in Lagoons

The circulation in individual reef lagoons may be forced by some or all of the current mechanisms described previously. In the extensive open lagoon between the shore and the barrier reef in the Great Barrier Reef, steady drift currents due to wind stress and pressure gradients, and periodic currents due to tides and continental shelf waves, all contribute to the water circulation. In the New Caledonia lagoon, about 20 × 80 km long inside a narrow barrier reef, the tide appears to be the main contributor to water circulation during light wind conditions. During strong southeast trade winds the wind stress superimposes a general northwest motion over the barrier reef and across the lagoon.

Within the Great Barrier Reef, individual reefs form partial obstacles to the general flow — "partial" because, except at very low water,

some flow occurs continually over the coral reefs. Eddies often form downstream of reefs, particularly during flows associated with tidal currents. Such eddies can increase mixing on a small scale (tens to hundreds of meters) as well as form closed volumes in which plankton can be held for hours or longer. Shedding of eddies behind reefs probably does not occur very often, because flow speeds are not great enough.

For the roughly circular lagoons within individual reefs in the Great Barrier Reef, again the drift and periodic currents contribute to the circulation together with inflow due to wave-overtopping. Studies within atoll lagoons have demonstrated that in addition to inflow due to ocean currents, tides, and wave-overtopping, wind stress causes downwind flow in the upper layer at speeds of about 3% of the wind speed while a compensating upwind flow develops in the deeper water.

Residence times for water within lagoons cover a wide range. For lagoons of 2–10 km diameter in the Great Barrier Reef, times of 0.5 to 4 days have been estimated, for Bikini Atoll 40 to 80 days, and for very shallow lagoons such as at Fanning Atoll (18 km long but only a few meters deep) periods of up to 11 months were estimated. Rougerie (1986) estimated residence times in the New Caledonia lagoon as 2 to 28 days, depending on the particular area and the runoff, wind, and tide characteristics.

S8.10. ADJACENT SEAS

S8.10.1. General Inflow and Outflow Characteristics

Adjacent seas affect the open ocean's stratification and circulation through water mass transformation. Transformation can be from dense to light water (as in the Black Sea and Baltic, where fresh water is added within the sea, greatly reducing the salinity, Chapter 9), from light to dense (as in the Nordic Seas and

the Mediterranean Sea, where there is large cooling and evaporation, Chapter 9), or due to vigorous mixing (as in the Indonesian passages, Chapter 11).

Exchanges between basins (inflow and outflow) can be principally separated in the vertical or in the horizontal directions (Figure S8.18). Adjacent seas that are separated from a larger basin by a narrow strait usually have vertically stratified exchange, with inflow in one layer and outflow in a layer of a different density. The inflow and outflow "layers" are separated by an interfacial layer within which vigorous vertical mixing modifies both the inflow and outflow. The Mediterranean, Black, and Baltic Seas, discussed in the following sections, have this type of exchange. Other examples include the Red Sea and Persian Gulf in the Indian Ocean (Section 11.6 and Section S8.10.7 below). For the Mediterranean, Red Sea and Persian Gulf, inflow is in the upper layer and outflow in the lower layer, with a density increase within the sea. In the Black and Baltic Seas, inflow is in the lower layer and outflow is in the upper layer, with a density decrease within the sea.

When the exchanges between basins can occur over a much broader region than just a narrow strait, the inflow/outflow geometry can be more horizontal, with water of one density entering in one region and transformed water exiting in another (Figure S8.18b). The inflow and outflow might adjoin each other, or occur through separate passages. The Caribbean Sea and Gulf of Mexico (Section 9.3.1) are of this type as are Fram Strait between Greenland and Spitsbergen (Chapter 12); the Indonesian passages (Section 11.5); and the Bering, Okhotsk, and Japan Seas (Sections S8.10.5 and S8.10.6).

Many exchanges are a mixture of horizontal and vertical. The exchange between the North Atlantic and North Sea (Section S8.10.4) is mostly horizontal, with inflow through Dover Strait and near the Shetland Islands and outflow along the
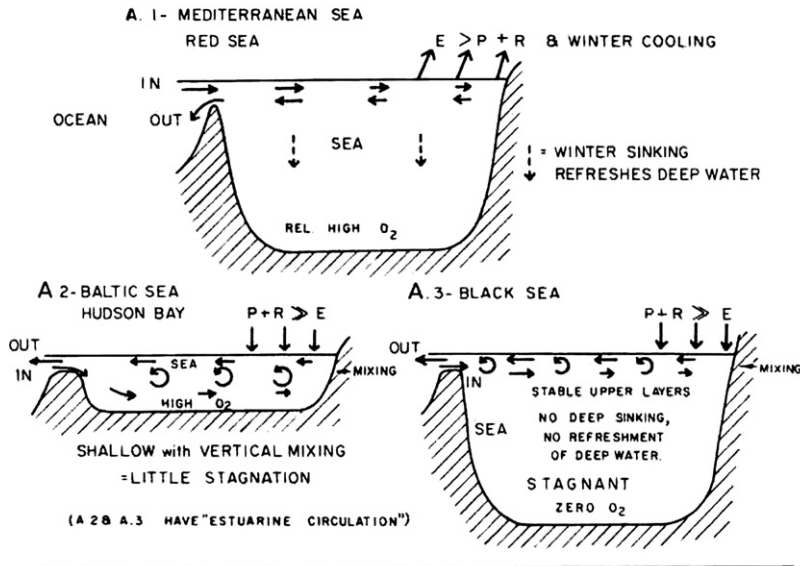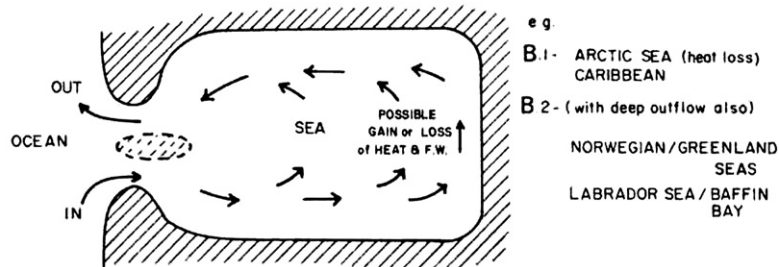
FIGURE S8.18 Schematic diagram of various types of circulation in seas adjacent to the oceans. (a) Vertically separated inflow and outflow, typified by the Mediterranean and Red Seas (surface inflow and subsurface outflow with transformation within the sea), Baltic Sea and Hudson Bay (subsurface inflow and surface outflow, with transformation within the sea), and Black Sea (subsurface inflow and surface ouflow, with no deep ventilation within the sea). (b) Horizontally separated inflow and outflow, typified by the Arctic Ocean and Caribbean Sea and also by the North Pacific marginal seas (surface inflow and surface outflow, usually through a different strait from the inflow), and by the Nordic Seas, Labrador Sea/Baffin Bay, and also the Persian Gulf (surface inflow and both surface and subsurface outflow).

Norwegian coast. But there is also inflow of saline water within the Norwegian Trench, beneath the fresher outflow along the Norwegian coast. For the Nordic Seas exchange with the North Atlantic, the exchange is mostly horizontal, with generally less dense Atlantic Water (AW) entering the Nordic Seas along the eastern boundary in the Norwegian Atlantic Current, and denser outflow occurring across each of the three main deep sills. However, the easternmost of these outflows, over

the Faroe-Shetland Ridge, is beneath the north-ward inflow of AW.

S8.10.2. Mediterranean Sea

The Mediterranean Sea (Figure S8.19) is a nearly enclosed marginal sea in the eastern North Atlantic, connected to the Atlantic through the Strait of Gibraltar, which has a sill depth of 284 m. The maximum depths within the sea are about 3400 m in the western basin and 4200 m in the eastern, separated by the Strait of Sicily, which is 430 m deep. The Mediterranean is connected to the Black Sea in the
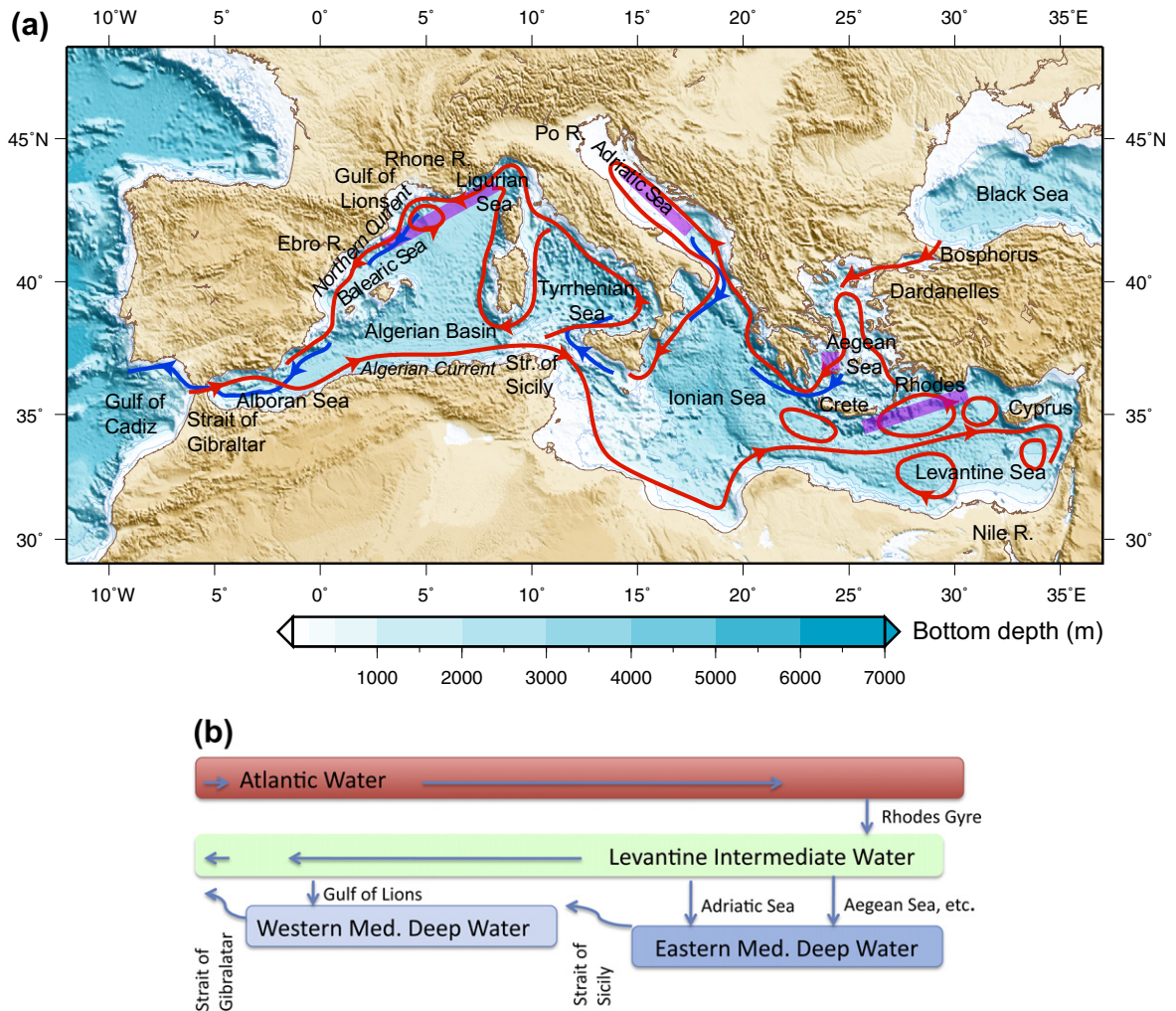
FIGURE S8.19 Mediterranean Sea. (a) Surface circulation schematic. Principal features are in red. *After Millot & Taupier-Letage (2005) and Robinson et al. (1991)*. Blue shows dense flow direction through the straits and away from formation areas, which are roughly indicated with purple. Etopo2 topography (m). *Source: From NOAA NGDC (2008)*. (b) Schematic of overturning circulation (surface, intermediate, and deep layers); curved arrows indicate that only the lighter part of the layer can flow over the sill.

northeast through the Dardanelles and Bosporus.

The tidal range in the Mediterranean is small, decreasing from 0.8 m at Gibraltar in the west to 0.4 m at Port Said in the east (to as low as 0.2 m along the French coast in the north). Sea level decreases in a northeasterly direction by about 0.7 m from the African coast to the Aegean Sea.

The Mediterranean Sea is the prototype of a "negative" basin in terms of water balance (Section 5.3.1), with evaporation exceeding precipitation and runoff. There is also net cooling within the sea. Therefore, the outflow from the Mediterranean is denser (saltier and cooler) than the inflow. The sea is well ventilated to its bottom as a result. The Mediterranean Sea has a profound impact on North Atlantic water properties because of the high salinity and density of its outflow. While the Mediterranean contributes only about one-third of the net evaporation of the Atlantic Ocean, its cooling of the saline surface waters allows them to sink to depth in the Atlantic, which is important for the entire North Atlantic Deep Water formation process.

S8.10.2.1 Exchange at the Strait of Gibraltar

The net exchange through the Strait of Gibraltar is small, on the order of 0.7 Sv (Bryden, Candela, & Kinder, 1994). The salinity difference between the Atlantic inflow in the surface layer and Mediterranean outflow below is large: 2.3 psu (from 36.1 to 38.4 psu). The inflow temperature is strongly seasonal, but averages around 15–16°C, hence a potential density of $s_q = 26.6$ to 26.8 kg/m^3. The temperature of the outflow is around 13.3 °C, so the potential density of the outflow is about 28.95 kg/m^3 (Figure 9.23b).

The flow through the Strait of Gibraltar is hydraulically controlled and modulated by tides (Armi & Farmer, 1988). Minimum sill depth is at the Camarinal Sill, while the minimum horizontal constriction is farther to the east, at Tarifa Narrows; both affect the outflow. The interface depth between the AW and outflowing Mediterranean Water is about 100 m at the sill, and slopes downward to almost 250 m depth on the Atlantic side (Bray, Ochoa, & Kinder, 1995). This downward slope is typical of hydraulically supercritical flow. The interface also slopes upward toward the northern side of the strait because of the Coriolis force, so the saltiest, densest water is banked to the north (Figure 9.23a).

The saline Mediterranean Water at the Strait of Gibraltar is one of the densest water masses in the world ocean; it is denser than the various Nordic Seas Overflow Waters (NSOW) at their overflow sills. However, instead of sinking to the bottom of the North Atlantic like the NSOW, the Mediterranean Water equilibrates at about 1200 m depth due to the difference in the stratification of the entrained waters for these two overflows (Price & Baringer, 1994; Figure S7.6b). The warmth of the Mediterranean outflow also means that it compresses less than NSOW as both descend to high pressure; in terms of potential density referenced to 4000 dbar, the NSOW is actually denser than the Mediterranean outflow.

S8.10.2.2 Circulation of the Mediterranean Sea

The horizontal and vertical circulations in the Mediterranean Sea are strongly affected by the basin geometry, which is separated into western and eastern basins by the Strait of Sicily and which has a saddle depth of about 430 m (Figure S8.19). The general sense of mean circulation in the Mediterranean Sea is cyclonic. Surface water enters from the North Atlantic through the Strait of Gibraltar. Within the Alboran Sea close to the strait, the circulation is anticyclonic (Alboran gyre), but then becomes cyclonic as the AW flows into the Algerian Basin, following the North African coastline. This eastward coastal flow is called the Algerian Current. The flow splits at the Strait of Sicily into a branch that continues eastward through the strait and

a northward branch feeding the cyclonic western Mediterranean circulation. The mean westward flow along the northern side can be called the Northern Current (Millot, 1991).

In the eastern Mediterranean, the Adriatic and Aegean circulations are each cyclonic. Circulation in the Levantine Basin is more complex, with a quasi-permanent, meandering eastward jet in mid-basin (the mid-Mediterranean or mid-Levantine jet; e.g., Robinson et al., 1991 and Özsoy et al., 1991). South of the jet, there are quasi-permanent, anticyclonic, sub-basin-scale gyres. North of the jet, there are cyclonic, sub-basin-scale gyres. Of the several commonly occurring gyres, the cyclonic Rhodes gyre between Crete and Cyprus is singled out here, as it is the site of Levantine Intermediate Water (LIW) formation (see later in this section).

The Mediterranean circulation is markedly time dependent. In the western Mediterranean, the Algerian Current regularly spawns large (100−200 km) anticyclonic mesoscale features, while the Northern Current region is also eddy-rich, although the features are not as coherent (Millot, 1991). In the eastern Mediterranean, the sub-basin-scale anticyclonic and cyclonic gyres are strongly time dependent (Özsoy et al., 1991; Robinson et al., 1991).

The mean horizontal circulation in the Mediterranean at both intermediate and deep levels is cyclonic, similar to the surface circulation (Millot & Taupier-Letage, 2005).

Transports of the main currents in the Mediterranean are on the order of 1 to 3 Sv. That is, the mean circulation is on the order of the exchange through the Strait of Gibraltar, and does not reach the strength of the open North Atlantic currents.

The vertical circulation of the Mediterranean is best described in terms of its water masses (Figure S8.19b and Section S8.10.2.3). AW flows in through the Strait of Gibraltar and circulates at the surface through the Mediterranean. In the eastern Mediterranean, LIW is formed in the vicinity of the Rhodes Gyre and then spreads cyclonically at mid-depth (200−600 m). LIW is the source of the deep waters in both the eastern and western Mediterranean. LIW and the lighter part of the Eastern Mediterranean Deep Water flow back to the west through the Strait of Sicily beneath the eastward flow of AW. This joins the Western Mediterranean Deep Water (WMDW). Outflow through the Strait of Gibraltar originates in the Northern Current along the coast of Spain and is composed of LIW and the upper part of the WMDW.

S8.10.2.3 Properties and Water Masses Within the Mediterranean Sea

The Mediterranean is a saline, warm, well-ventilated basin. Due to prevailing dry northwest winds and frequent sunny days, there is a large excess (about 100 cm/year) of evaporation over precipitation in the eastern part of the Mediterranean Sea. The high temperatures and salinities are surpassed only in the Red Sea. Salinity ranges from 36.1 psu, in the entering AW, to 39.1 at the surface in the eastern Mediterranean. Bottom temperatures are above 12.5°C even at 4000 m (Wüst, 1961) and have become warmer (Klein et al., 1999). Bottom water densities exceed $s_q = 29.25$ kg/m^3 due to the high salinity and deep oxygen exceeds 200 μmol/kg. These properties differ greatly from those at the same depth in the adjacent North Atlantic, which are 2.4°C, 34.9 psu, and $s_q = 27.8$ kg/m^3.

The nomenclature for Mediterranean water masses has varied. An official list of names and acronyms is maintained by CIESM (2001). We limit our discussion to four primary water masses: AW in the surface layer; LIW in the intermediate layer; and two dense waters, WMDW and the denser Eastern Mediterranean Deep Water (EMDW). LIW is formed in the northern Levantine Basin, off the south coast of Turkey near the island of Rhodes. The Deep Waters are formed at the northern edges of the basins, chiefly in the Gulf of Lions in the western

basin (WMDW) and in the southern Adriatic and in the Aegean (EMDW).

LIW is recognized throughout the Mediterranean by a subsurface vertical maximum of salinity between 200 and 600 m (Figure S8.20; Wüst, 1961). At formation, LIW salinity is greater than 39.1 psu and its temperature is around 15°C. After passing westward through the Strait of Sicily its core becomes colder (13.5 °C), fresher (38.5), slightly less dense, and somewhat deeper than in the eastern Mediterranean.

LIW formation was observed in the cyclonic Rhodes Gyre in early 1995 (Malanotte-Rizzoli et al., 2003). Deep convection to 900 m occurred in this gyre (Figure S8.21), acting as a classic convective chimney (Section 7.10). The dense
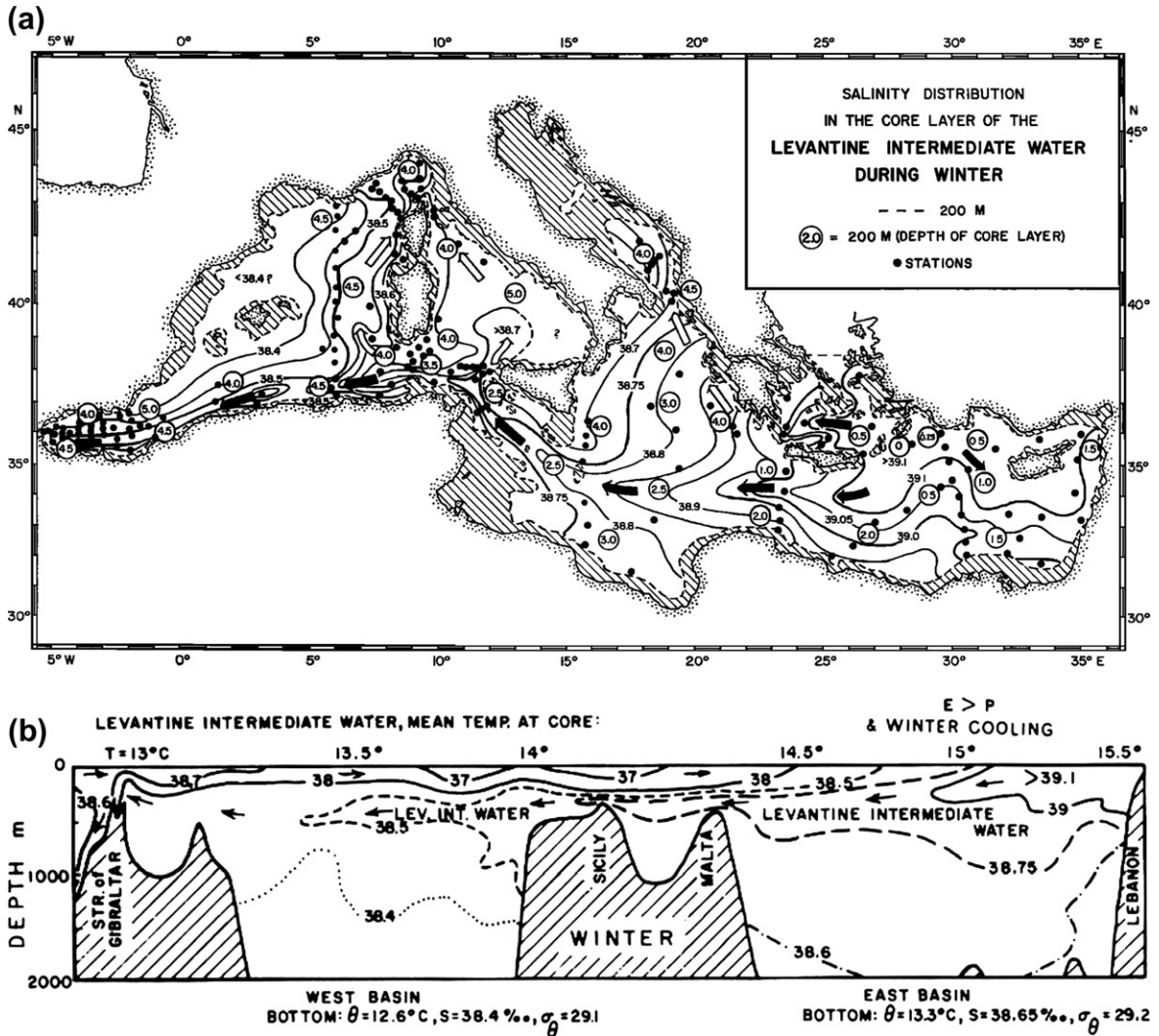

FIGURE S8.20 (a) Salinity at the vertical salinity maximum characterizing LIW. *Source: From Wüst (1961).* (b) Longitudinal salinity section in winter to show the LIW.
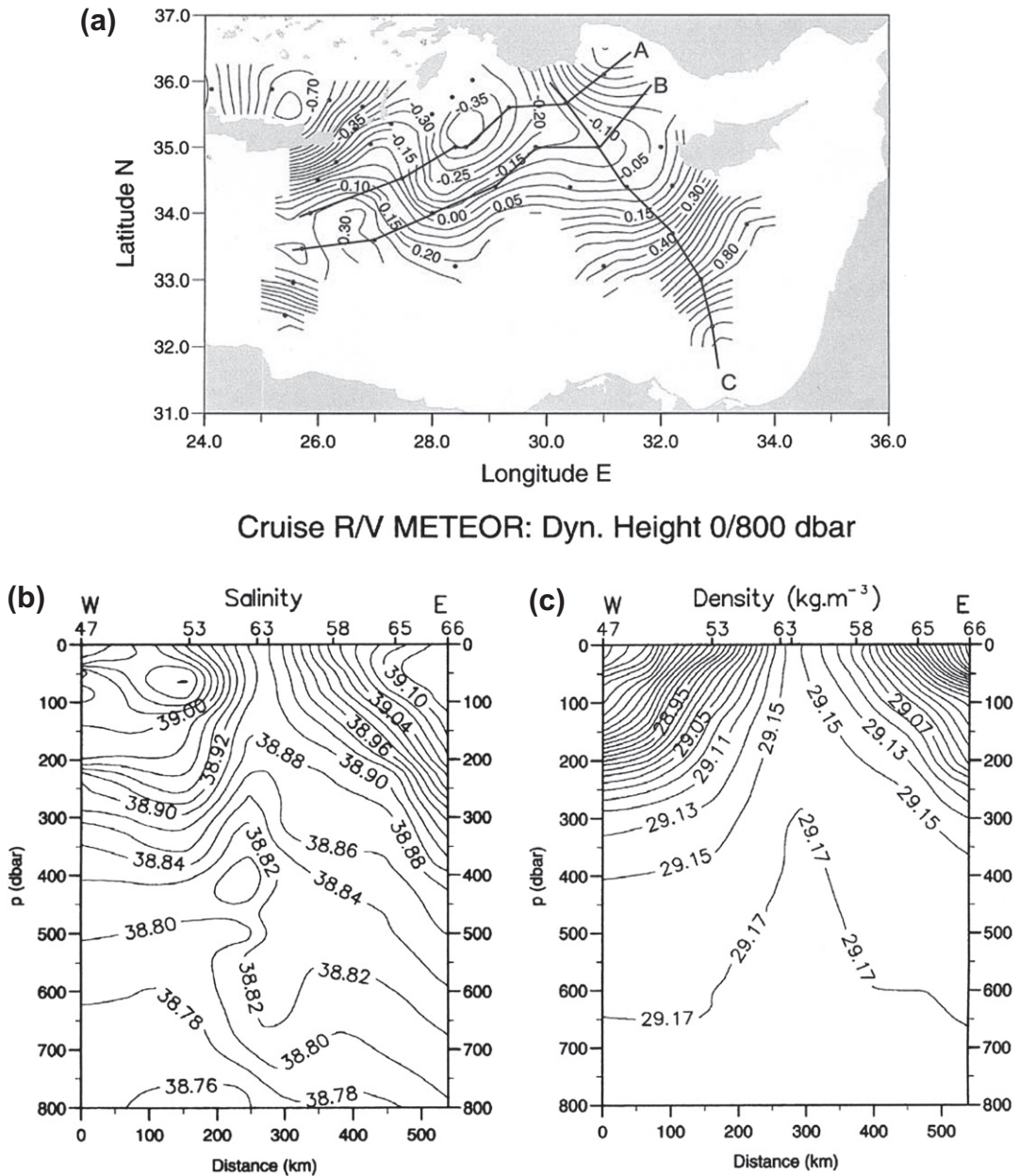
FIGURE S8.21   Eastern Mediterranean convection. Formation of dense water in the Levantine Basin in January 1995. (a) Surface dynamic height relative to 800 dbar. The cyclonic low centered at 28°30′E, 35°N is the Rhodes gyre. (b) Salinity and (c) potential density s_q along section A. LIW is the salinity maximum at 50–100 m. The convective chimney in the center is forming a deep water. *Source: From Malanotte-Rizzoli et al. (2003).*

water in the chimney in that year was a newly identified deep water, rather than LIW. New LIW was the shallow salinity maximum on the outside of the gyre (right and left at 50−100 m depth in Figure S8.21b,c). LIW spread much farther into the eastern Mediterranean at the end of that winter than did the new deep water, which was trapped in the Rhodes Gyre.

The Deep Waters originate at several locations along the northern coast through winter cooling of the widespread high salinity LIW. In the Adriatic and Aegean, cold winter outbreaks with intense winds (the "Bora") create EMDW from LIW. The Adriatic has historically been the site of the densest formation (Schlitzer et al., 1991). However, changes in winter conditions shifted the densest water production to the Aegean in the 1980s, and then back to the Adriatic in the 1990s (Klein et al., 2000). The presence of EMDW affects the properties of new LIW in the eastern Mediterranean.

In the western Mediterranean, dense water formation contributing to WMDW occurs primarily in the Gulf of Lions in a sub-basin-scale cyclonic gyre (Figure S8.22), in response to cold, dry winter winds (the "Mistral"). The first observations of the classic stages of deep convection (preconditioning, convective mixing and spreading; Section 7.10.1) were made here in 1969 (MEDOC Group, 1970; Sankey, 1973). Deep convection has occurred reliably in this region in many other years within a cyclonic dome of about 100 km scale. Dense water properties here are around 12.8°C, 38.45 psu, and $s_q = 29.1$ kg/m^3 (Marshall & Schott, 1999). Thus WMDW is not as dense as EMDW, but the Strait of Sicily blocks the densest EMDW from flowing into the western Mediterranean. Thus the deep water of the western Mediterranean is a mixture of local Gulf of Lions dense waters and the shallower part of EMDW.

Water mass properties and formation rates in the Mediterranean are demonstrably affected by the North Atlantic Oscillation and by the warming and drying trends of global climate change

(Section S15.6). Because the sea is relatively small, these changes affect the relative balance and properties of the different deep and intermediate waters. The net effect is observed in changes of salinity and temperature of the outflow at the Strait of Gibraltar. This has affected Mediterranean Water properties within the North Atlantic (Potter & Lozier, 2004).

S8.10.3. Black Sea

The Black Sea is an almost completely isolated marginal sea with a maximum depth of over 2200 m. It is connected to the northeastern Mediterranean Sea through the narrow Bosphorus and Dardanelles, which have depths of only 33 and 70 m, respectively (Figure S8.23). The small Sea of Marmara lies between the two straits. Inflow from the Mediterranean is more saline and denser than the fresh outflow from the Black Sea. The Black Sea thus represents a classic estuarine circulation with inflow at the bottom and outflow at the surface in the straits; it is a "positive sea" because it has a net input of freshwater (Section 5.3.2). The Black Sea is also a prototypical anoxic sea with no dissolved oxygen below the pycnocline because of the very long residence time of its deep water. Black Sea physical oceanography was reviewed by Özsoy and Ünlüata (1998) and Oguz et al. (2006).

The surface circulation of the Black Sea is cyclonic overall, with a cyclonic gyre in each of the west and east basins, including cyclonic eddies (Figure S8.23a and Oguz et al., 2006). A Rim Current circulates around the exterior, roughly following the continental shelf break. Its maximum velocity is 50−100 cm/sec at the surface. Inshore of the Rim Current is a series of anticyclonic eddies or small gyres that connect the coastal regions with the cyclonic circulation (light contours in Figure S8.23a). The whole is dominated by time-dependent eddies and seasonal changes in circulation.
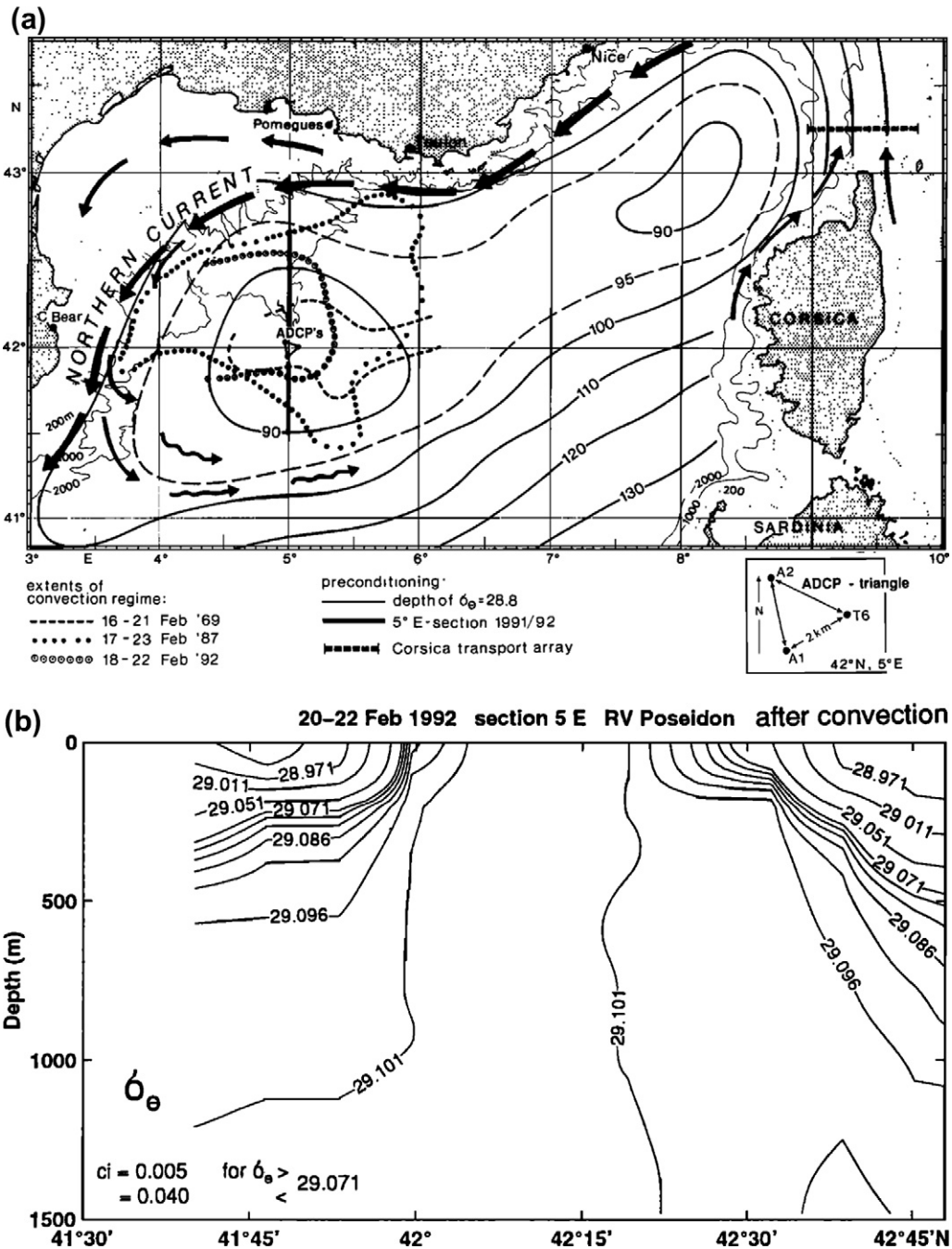
FIGURE S8.22 Western Mediterranean convection. (a) Deep convection region in the Gulf of Lions for three winters. Circulation (arrows) and isopycnal depth (m) showing cyclonic doming. (b) Potential density through the convection region in February 1992. *Source: From Marshall and Schott (1999).*

The narrowness and shallowness of the passages between the Black Sea and Mediterranean result in high current speeds and vertical shear. The consequent turbulence causes vertical mixing between the inflow and outflow layers. Therefore the surface water that leaves the Black Sea with a salinity of about 17 psu reaches the Mediterranean with its salinity increased to about 30 psu, while the salinity of 38.5 psu of incoming subsurface Mediterranean water is reduced to about 34 psu by the time that it reaches the Black Sea.

Exchange with the Mediterranean includes inflow on the order of 300 km³ yr⁻¹ (300 km³ yr⁻¹ is equal to 9.5×10^3 m³sec⁻¹, hence 0.0095 Sv) and outflow of the order of 600 km³ yr⁻¹ (Oguz et al., 2006). The higher outflow is due to net freshwater input. Evaporation and precipitation within the Black Sea are each on the order of 300 km³ yr⁻¹ each, so they are nearly
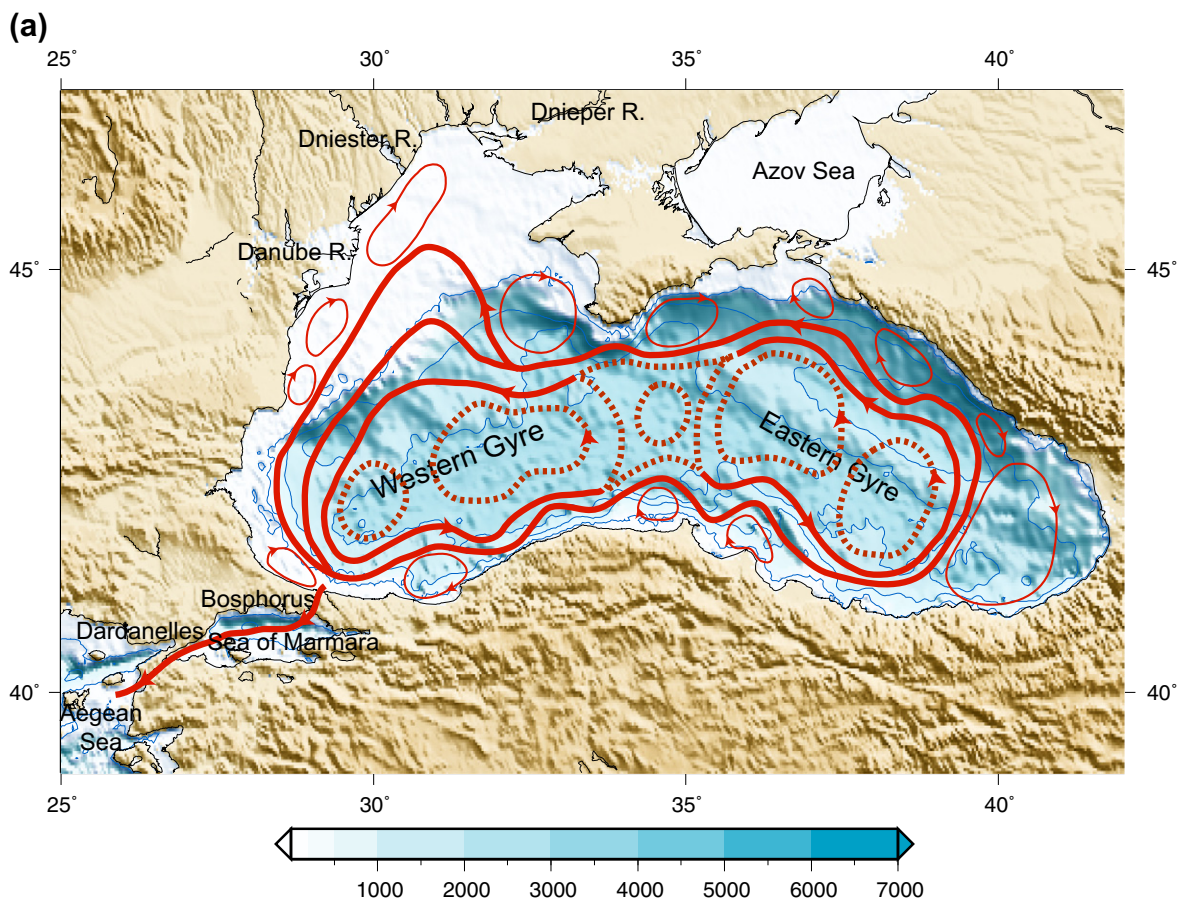

(a)

FIGURE S8.23 Black Sea. (a) Surface circulation schematic. Heavy contours: principal circulation. Light contours: shelf circulation. Dashed contours: eddy-like circulation in interior. Blue: subsurface inflow through the Dardanelles and Bosphorus. *After Oguz et al. (2006), with Etopo2 topography from NOAA NGDC (2008).* (b) Water properties in the upper 200 m in the Black Sea, 1988. *Adapted from Murray et al. (1989).* (c) Overturn and transport balances (km³ yr⁻¹). *Source: From Oguz et al. (2006).*
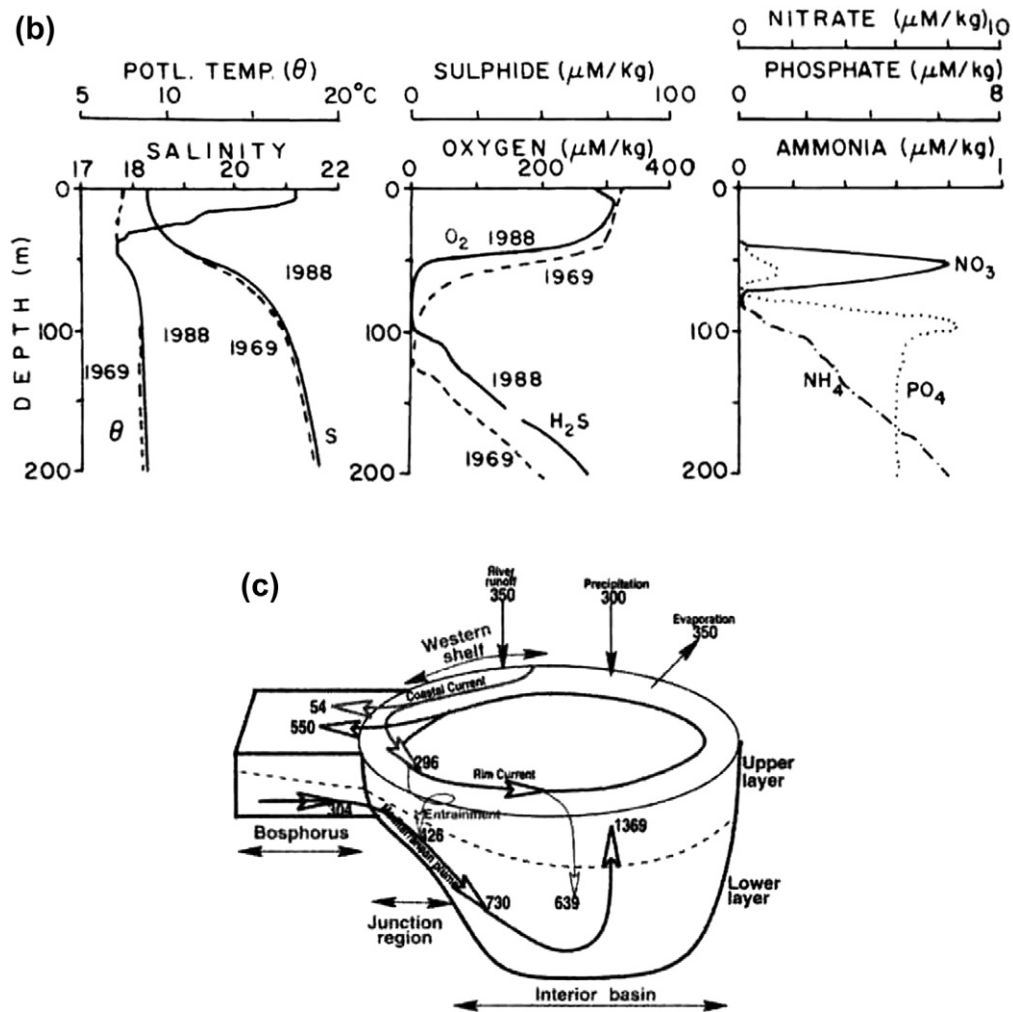
FIGURE S8.23   (*Continued*).

balanced. Inflow from the large rivers, including the Danube, Dniester, and Dnieper in the northwest, is also on the order of 300 km^3 yr^{-1}. Thus without the river inflow, salinity in the Black Sea would be nearly neutrally balanced. In Section 5.3.2, we calculated a residence time for the Black Sea of 1000 to 2000 years.

As a result of the net input of freshwater and the long residence time, the Black Sea is one of the world's major brackish (low salinity) seas.

A halocline between 50 and 100 m separates the fresher surface layer from the subsurface water column (Figure S8.23b). The sharp halocline/pycnocline separates the upper low-salinity, oxygenated (oxic) water from the deeper oxygen-free (anoxic) water.

A subsurface temperature minimum of <8 °C near 100 m is called the *Cold Intermediate Layer*. It is most likely a remnant of the winter surface mixed layer. Because the surface layer is so

fresh, this density structure is stable; it is similar to the subpolar structures found in the northern North Pacific and parts of the Southern Ocean. The Deep Water in the Black Sea has a salinity of 22.3 psu and potential temperature of 8.9 °C.

The salinity structure and isolation of the deep Black Sea produce interesting double diffusive and deep geothermal convective features. The overall vertical structure is diffusive, with colder, fresh water in the Cold Intermediate Layer overlying warmer, saltier water below the pycnocline (Özsoy & Ünlüata, 1998; Kelley et al., 2003). Inflowing salty Mediterranean water enters the pycnocline and below in intrusions that are double diffusive. Weak geothermal heating at the bottom of the Black Sea, along with the long residence time, creates a very thick (>450 m) convective bottom layer, rivaled only in the deep Arctic (Section 12.5.3; Timmermans, Garrett, & Carmack, 2003).

Over geological time, the Black Sea has varied from being fresh (as recently as 7000 years ago), to moderately saline. As global sea levels rose and fell during glacials and interglacials and river outlets changed location, the exchange between the Black Sea and Aegean may have reversed direction and even ceased because the Bosphorus and Dardanelles are so shallow. There is an ongoing paleoclimate debate about whether overflow in through the Bosphorus 5600 years ago created a sea level rise of tens of meters and massive flooding around the Black Sea or milder changes (Giosan, Filip, & Constatinescu, 2009).

The considerable river runoff into the Black Sea has decreased by 15% in the last several decades due to the diversion of the river water for agricultural purposes. Observations in 1988 compared with 1969 (Figure S8.23b) showed higher salinity by about 0.1 psu, ascribed to the change in runoff (Murray et al., 1989). The lower temperature in the surface layer in Figure S8.23b is due to a month of observation in the two years.

S8.10.4. Baltic and North Seas

The North Sea is the semi-enclosed, shallow, continental shelf sea of about 100 m depth between the British Isles, Norway, and Europe; it is connected to the open North Atlantic through a broad region between Scotland and Norway at 61°−62°N and through Dover Strait (Figure S8.24). The Baltic Sea is the nearly enclosed sea east of Denmark. The Baltic is connected to the North Sea at its southwest end through a complex of passages with a sill depth of 18 m, leading to the Kattegat and the North Sea. The Kattegat is the small sea between Denmark and Sweden. The Baltic, which includes the Gulf of Bothnia to the north and the Gulf of Finland to the east, is the largest area of brackish (nearly fresh) water in the ocean system. It has irregular bottom topography, with a mean depth of 57 m, and a number of basins of which the deepest is 459 m deep.

The physical oceanography of both seas was reviewed in Rodhe (1998) and Rodhe, Tett, and Wulff, (2006). Since 1992, the Baltic Sea has been the focus of an intensive hydrological cycle study called "Baltex" (the Baltic Sea Experiment); as an outcome of the study, Leppäranta and Myrberg (2009) provided a thorough overview of Baltic Sea physical oceanography.

Surface salinity clearly illustrates the connection of the North Sea to the open ocean and the much greater isolation of the Baltic (Figure S8.24b). Surface salinity in the North Sea is close to oceanic values, with a tongue of high salinity (>35) entering from the north. Through the Kattegat and into the Baltic, there is an enormous decrease, with salinity in the southern Baltic between 7 and 8 psu, dropping to less than 2 psu in the northernmost Gulf of Bothnia and easternmost Gulf of Finland.

The North Sea circulation is cyclonic, with most water entering and leaving across the continental shelf break in the north. The exchange transport is about 2 Sv. Properties

and circulation along the western side are strongly modulated by tides, which vertically mix the inflowing waters, with some dilution of salinity due to river inflow. Inflow from the Baltic through the Kattegat introduces much lower salinity waters into the North Sea; the northward flow along the coast of Norway that feeds the outflow is strongly stratified in salinity as a result. Its circulation is estuarine because of this net freshwater input.

The Baltic Sea, like the North Sea, has an estuarine circulation (Figure S8.24c) with the upper layer outflow in the Kattegat having a salinity of 20 psu and the bottom layer inflow having a salinity of 30−34 psu. Large-scale meteorological conditions can override the estuarine circulation and result in full depth inflow or outflow at times.

The mean circulation in the Baltic Sea is weak and cyclonic with mean surface currents of about 5 cm/sec and no major stable features. The complicated geography of this sea creates a complex deeper circulation. However, the circulation is extremely time dependent and
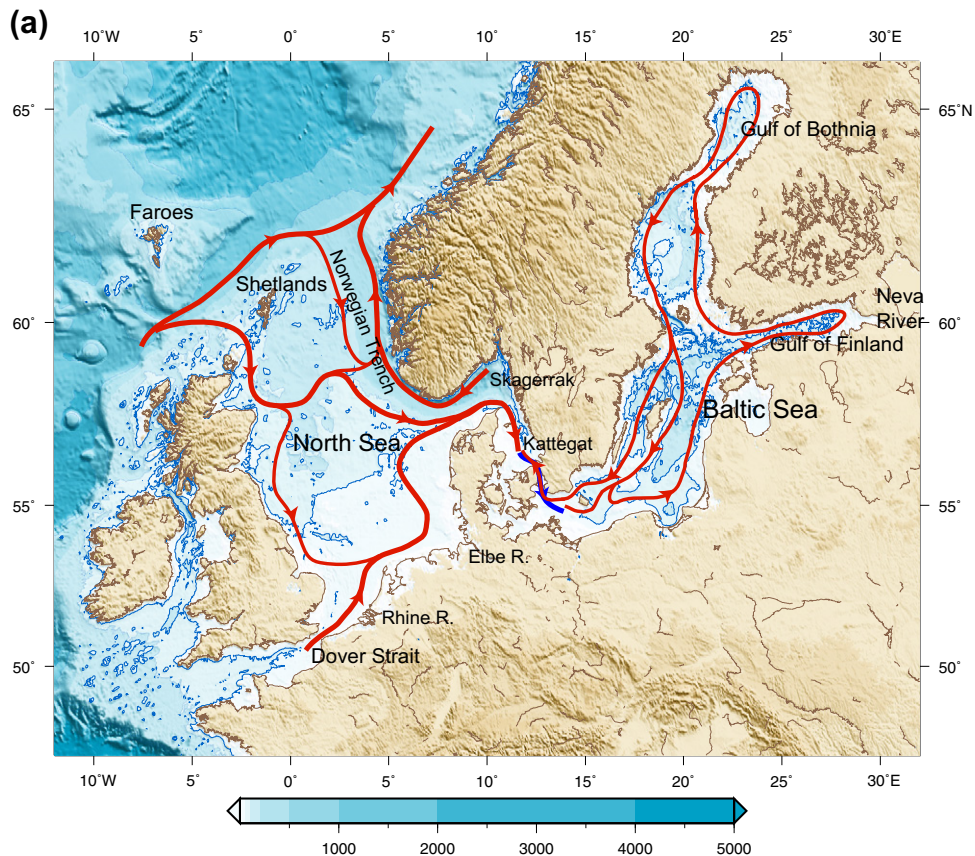
FIGURE S8.24 North Sea and Baltic Sea. (a) Surface circulation schematic. *After Winther and Johannessen (2006) and Leppäranta and Myrberg (2009) with Etopo2 topography from NOAA NGDC (2008).* Blue indicates subsurface flow through the Kattegat. (b) Surface salinity in August in the Baltic and North Seas. *Source: From Rodhe (1998).* (c) Physical processes in the Baltic. *Source: From Winsor, Rodhe, and Omstedt. (2001).*
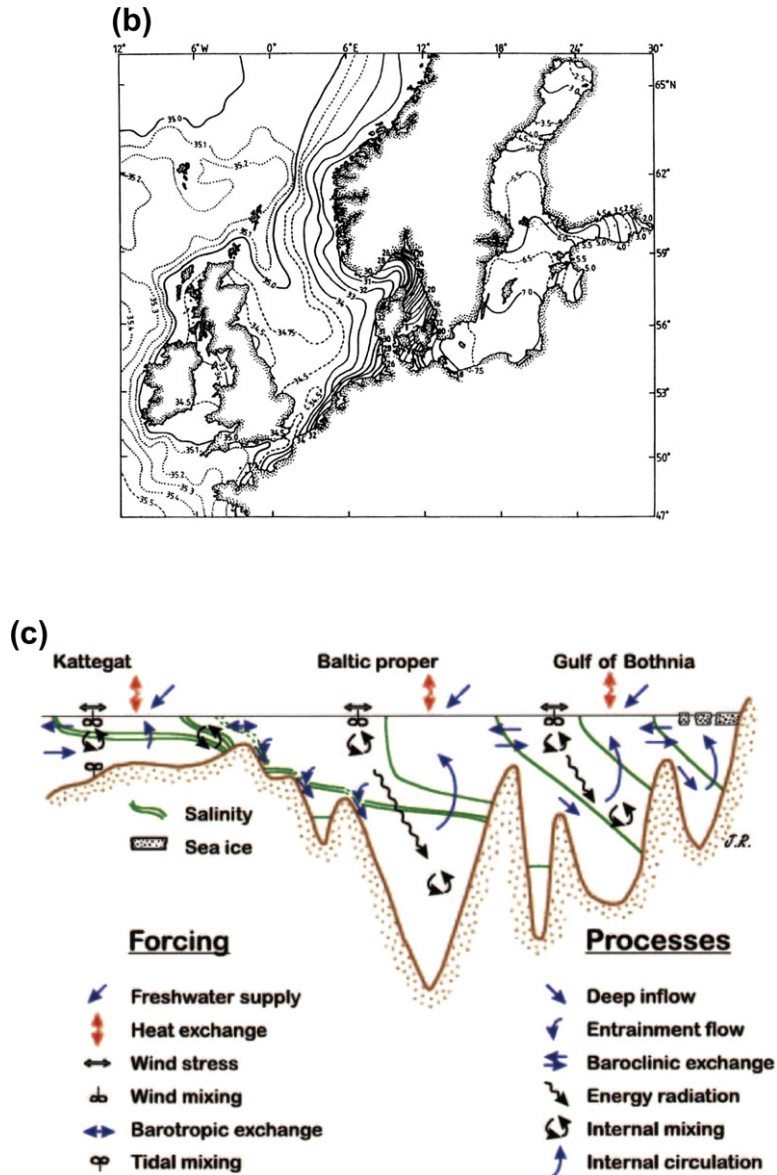
(b)

(c)

FIGURE S8.24 (*Continued*).

strongly coupled to the wind (through the Ekman layer) because of the shallowness of the sea; currents can reach 50 cm/sec in the open sea and up to 100 cm/sec in straits during storms (Leppäranta & Myrberg, 2009).

The very low salinity of the Baltic Sea results primarily from river runoff and a long residence time of waters within the Baltic of more than 30 years (see Section 4.7). Evaporation and precipitation are estimated to be nearly

equal at about 47 cm/year. The freshwater budget is always positive, even on a monthly level, because of the river inflows, which are equivalent to 123 cm of water over the whole area of the Baltic Sea. The bulk is due to the Neva River into the Gulf of Finland, equivalent to 400 cm/year over that gulf, and 170 cm/year to the Gulf of Bothnia, with significant year-to-year variations.

The Baltic is basically a two-layer system, with a well-mixed upper layer (in terms of salinity) that is 30— 50 m deep in the south, increasing to 60—70 m in the central Baltic. The upper layer temperature in summer is over 10 °C with a thermocline at 15—20 m, which is significantly shallower than the halocline. Surface layer salinities are 6— 8 psu while the deeper waters are usually 10— 13 psu, sometimes exceeding 17 psu in the south when large inflows occur. These bursts of inflow typically occur no more than once a year, with the strongest events sometimes separated by a decade or more (Jakobsen, 1995). Surface salinity in the gulfs is even lower at 2—7 psu. Dissolved oxygen reaches 100% saturation in the surface layers, but is relatively low in the deep water, with variations on a decadal timescale related to variations of inflows from the Kattegat. Anoxic conditions occur in many of the deeper Baltic basins where the residence times are several years.

Starting in January, sea ice forms in the north and east gulfs (Gulfs of Bothnia and Finland) along the coast. The ice often extends to mid-gulf but is less extensive in the central Baltic.

S8.10.5. Subtropical North Pacific Marginal Seas

Along the western boundary of the tropical and subtropical Pacific lies a set of marginal seas that interact differently with the open North Pacific circulation (Figure 10.1). From south to north, these are the South China Sea, the East China Sea, the Yellow Sea, and the Japan (or East) Sea. Farther to the north lie the subpolar Okhotsk and Bering Seas (Section S8.10.6). Wind forcing for the southern part of this region is strongly monsoonal, with the seasonality weakening to the north. These seas are connected through shallow straits or are located on the continental shelf; the net transport exchanges between them and with the Kuroshio, which lies in deep water to the east, therefore are limited and of the order of 2 Sv.

The *South China Sea* circulation is highly seasonal, driven by the Asian monsoon. Inflow from the Pacific occurs throughout the year through Luzon Strait between Luzon and Taiwan; these are Kuroshio waters. Exit is northward through Taiwan Strait, between Taiwan and the continent, also throughout the year. The exchange rate is approximately 2 Sv (Xue et al., 2004). Within the South China Sea, the summer circulation is mostly anticyclonic, driven by southwesterly winds, while in winter it is mostly cyclonic, driven by northeasterly winds (Hu, Kawamura, Hong, & Qi, 2000). In Figure 10.1, only the cyclonic winter circulation is depicted. The western boundary current along Malaysia, Vietnam, Hainan, and southern China reverses from southward in winter to northward in summer. However, in the north, the South China Sea Warm Current flows northward through Taiwan Strait throughout the year, with maximum transport in summer when the full western boundary current complex is northward.

The *East China Sea* and *Yellow Sea* constitute the broad continental shelf region that lies east of China, north of Taiwan, and west and south of Korea. The eastern edge of the continental shelf is the effective western boundary for the North Pacific's circulation, hence for the Kuroshio, which flows northward along the continental slope. Flow enters the East China Sea from the South China Sea through Taiwan Strait in the Taiwan Warm Current. Exit is to the north into the Japan Sea through Tsushima Strait (Korea Strait) in the Tsushima Warm Current.

Within the Yellow Sea, the circulation is cyclonic and much stronger in winter than in summer due to the strong northerly monsoonal wind forcing (Naimie, Blain, & Lynch, 2001). This overall region also absorbs the major freshwater output from the Changjiang River (Yangtze River). Cross-shelf exchange with the Kuroshio modifies the properties of the East China Sea waters. The Bohai Sea, which is the gulf north of the Yellow Sea, forms sea ice in winter; this is the southernmost ice-covered region in the Northern Hemisphere.

The *Japan Sea* (East Sea) lies between Asia and Japan. It is deep with bottom depths exceeding 3000 m, but it is connected to the North Pacific and Okhotsk Sea only through shallow straits. Water enters the Japan Sea from the south through Tsushima Strait (140 m deep). The source of this warm, saline subtropical water is the East China Sea with some possible input from an onshore branch of the Kuroshio. The net transport into the Japan Sea is estimated at a little less than 2 Sv (Teague et al., 2006). Water exits from the Japan Sea mainly through Tsugaru Strait, between Honshu and Hokkaido (130 m deep). There is also small but important transport into the Okhotsk Sea through Soya Strait between Hokkaido and Sakhalin, and through the very shallow Tatar Strait far to the north, between Siberia and Sakhalin.

Within the Japan Sea, there are typical subtropical and subpolar circulations driven by Ekman downwelling in the south and upwelling in the north, and separated by a zonal subarctic front that is similar to the North Pacific's subarctic front. The northward subtropical western boundary current is the East Korean Warm Current. The subpolar western boundary current is the Primorye (or Liman) Current where it flows along the coast of Russia and the North Korean Cold Current where the flow intrudes southward along the Korean coast.

The Japan Sea circulation deviates from a typical open ocean gyre system because of its vigorous eastern boundary current, the Tsushima Warm Current, which flows northward along the coast of Honshu. This results from the "island effect," which is related to the wind forcing of the entire North Pacific circulation east of Japan with open straits on the southern and northern sides of the island (this is outside the scope of this text).

A principal role of the Japan Sea in the North Pacific circulation is to carry warm, saline subtropical water northward west of Japan, (cool and freshen it), and then expel the still-saline water north of the Kuroshio's separation point. This impacts details of formation of the salinity minimum of North Pacific Intermediate Water east of Japan (Section 10.9.2; review in Talley et al., 2006).

S8.10.6. Bering and Okhotsk Seas

The Bering and Okhotsk Seas are separated from the North Pacific by the long Aleutian and Kuril Island chains. The North Pacific's cyclonic subpolar circulation partially loops through these adjacent seas. The two seas are intrinsically part of the North Pacific's circulation, but the island chains create leaky barriers that partially support boundary currents and a large amount of mixing in the island passages due to tides. Both seas have sea ice formation and brine rejection processes in the winter that create denser shelf waters. Because the Okhotsk Sea has a salty external source of water from the Japan (East) Sea, through Soya Strait, its brine rejection process produces denser water than in the Bering Sea. The Bering Sea's special role is as a small conduit of Pacific waters to the Atlantic Ocean.

In the *Bering Sea*, cyclonic circulation enters from the Alaskan Stream beginning with the easternmost passages through the Aleutians; the principal deep inlet straits are Amchitka Pass at about the date line (1155 m), and Near Strait at 170°E (2000 m), just west of Attu Island (Stabeno & Reed, 1995). Most of the exit flow is through Kamchatka Strait (4420 m depth)

between Kamchatka and the Komadorskiy Islands with a smaller amount exiting to the Arctic through the shallow Bering Strait. The Bering Sea is well known for its vigorous eddy field that obscures much of the mean circulation in synoptic data (Reed, 1995). Flow around groups of islands in the Aleutian chain is anticyclonic and tidally driven.

Within the Bering Sea, the inflow from the central and eastern straits proceeds cyclonically, with the principal northwestward flow following the continental shelf topography as the *Bering Slope Current* (Kinder, Coachman, & Galt, 1975). When it encounters the Kamchatka boundary, the Bering Slope Current splits. The southward flow along the coast of Kamchatka is the East Kamchatka Current (EKC), which becomes the principal western boundary current for the North Pacific's subpolar gyre. This is joined by water circulating in the deeper basin of the Bering Sea, and exits to the North Pacific following the Kamchatka coast. The EKC outflow transport through Kamchatka Strait is 6–12 Sv (Stabeno & Reed, 1995).

The flow of water northward through Bering Strait to the Arctic Ocean is one of the principal pathways in the global overturning circulation, despite the shallowness of the strait (~50 m) and its small transport (~0.8 Sv; Roach et al., 1995). This is the only northern connection between the Pacific and Atlantic. The flow is relatively fresh (~32.5 psu) relative to global mean salinities and is thus one of the freshwater exits from the Pacific (Wijffels, Schmitt, Bryden, & Stigebrandt, 1992; Talley, 2008). The water flowing into Bering Strait comes from a western boundary flow, the Anadyr Current, which is the northward branch of the Bering Slope Current, and a warmer eastern boundary flow, the Alaskan Coastal Current, which is fed by cyclonic circulation around the broad Bering Sea shelf (Woodgate & Aagaard, 2005).

The *Okhotsk Sea* is connected to the North Pacific through the Kuril Island chain. It is the source of the densest water in the North Pacific, which contributes to the North Pacific Intermediate Water. The predominantly cyclonic circulation of the Okhotsk Sea enters through the northernmost strait close to the southern end of the Kamchatka peninsula (Kruzenshtern Strait, ~1400 m depth), and through Bussol' Strait, which lies in the center of the Kurils and is the deepest passage (~2300 m depth). Net outflow is mainly through Bussol' Strait, which, like the other straits, has bidirectional flow associated with anticyclonic flow around each island. The net transport in and out of the Okhotsk Sea is approximately 3–4 Sv (Gladyshev et al., 2003. This water is greatly modified within the Okhotsk Sea.

Within the Okhotsk Sea, the cyclonic circulation flows northward along the western side of Kamchatka as the *West Kamchatka Current*, and westward along the broad continental shelves on the northern Siberian boundary, where sea ice formation produces especially dense shelf waters (Section 10.9.2). The Amur River injects fresh water in the northwest. The complex then moves southward along the east coast of Sakhalin, as the *East Sakhalin Current*, which is a typical narrow western boundary current. Waters from the East Sakhalin Current enter the region south of Sakhalin, join an anticyclonic circulation there, and then head for Bussol' Strait. They are joined by eastward flow in the *Soya Current* along the northern coast of Hokkaido that enters the Okhotsk Sea from the Japan Sea through Soya Strait.

S8.10.7. Red Sea and Persian Gulf

Geographically, the Red Sea, west of the Arabian Peninsula, is a rift valley, resulting from the separation of Africa and the Arabian Peninsula, which is closed at the north and opens to the Gulf of Aden, Arabian Sea, and the Indian Ocean at the south through the narrow strait of the Bab el Mandeb (or Bab al Mandab; see Ross, 1983 in Ketchum). The depth averages 560 m, with maximum values

of 2900 m and a sill of about 110 m depth at the Bab el Mandeb in the south.

In contrast, the Persian or Arabian Gulf, east of the Arabian Peninsula, is shallow with a maximum depth of 105 m and average depth of 35 m (Swift & Bower, 2002). The Persian Gulf is connected to the Arabian Sea through the Strait of Hormuz (86 m deep) and the Gulf of Oman.

This brief introduction to these marginal seas is well complemented by the greater detail in Tomczak and Godfrey (1994).

A major aspect of the northwestern Arabian Sea is the high evaporation rate of approximately 100− 200 cm/year, while precipitation averages about 7−10 cm/year. There are no major rivers flowing into the Red Sea. The Tigris and Euphrates Rivers drain into the Persian Gulf, but their freshwater contribution is far smaller than the net evaporation.

The water structure in the Red Sea consists of a shallow upper layer and a thick deep layer separated by a thermocline/halocline at about 200 m depth. At the surface, the temperature in summer (June −September) is 26°−30°C, and in winter (October −May) it is 24−28°C. Below the thermocline the deep layer is nearly isothermal, at 21.6−21.8°C. The Red Sea is the most saline large body of ocean water, with surface layer values of 38− 40 psu (with higher values to 42.5 psu in the north) and deep water values of 40.5−40.6 psu. The deep water is formed by winter cooling in the north. The surface layer is saturated with dissolved oxygen, but the absolute values are low because of the high temperature (less than 175 μmol/kg). There is an oxygen minimum of 20−60 μmol/kg at 400 m below the thermocline/halocline, whereas the deep water below this has a content of 80−90 μmol/kg.

A schematic Red Sea mean circulation is presented in Figure S8.25a. The central Red Sea ocean surface pressure (sea level) is dominated by two highs with flanking lows in the north and south. Intermediate water forms in the northern low. All of the mean boundary
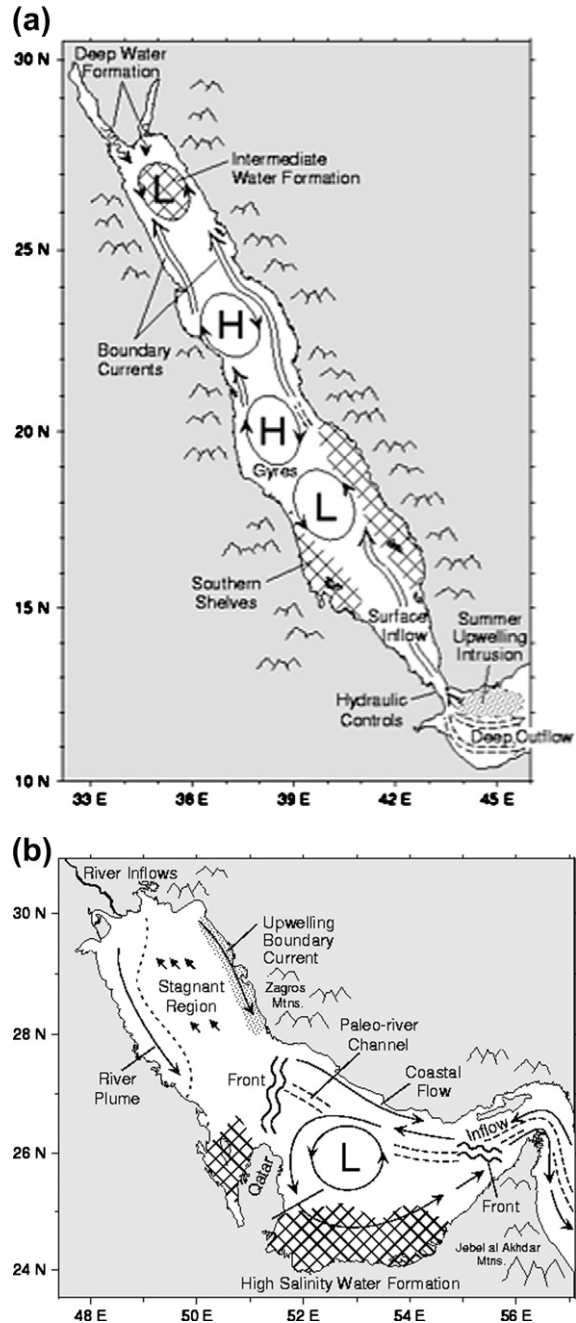
FIGURE S8.25 Schematic circulations: (a) Red Sea and (b) Persian Gulf. *Source: From Johns et al. (1999).*

currents flow to the north, reflecting the net thermohaline overturn in the Red Sea.

The Red Sea circulation's seasonal variation is related to the winds (Johns et al., 1999; Sofianos & Johns, 2003). In summer (Southwest Monsoon) the winds are to the south over the whole Sea (Figure S8.26); the surface flow is southward with outflow through the Bab el Mandeb, while there is a subsurface inflow to the north and weak outflow at the bottom through that strait. In the winter (Northeast Monsoon) the winds over the southern half of the Red Sea change to

northward; there is a northward surface flow over the whole of the Red Sea and a subsurface southward flow with outflow through the Bab el Mandeb. The residence time for the upper layer has been estimated at 6 years and for the deep water at 200 years.

Hot brine pools are found in some of the deepest parts of the Red Sea (Karbe, 1987). Very high temperatures of 58°C and salinities of 320 psu are due to hydrothermal activity. The heat flow up through the bottom is much greater than the world average of 4×10^{-2} W/m^2. The high
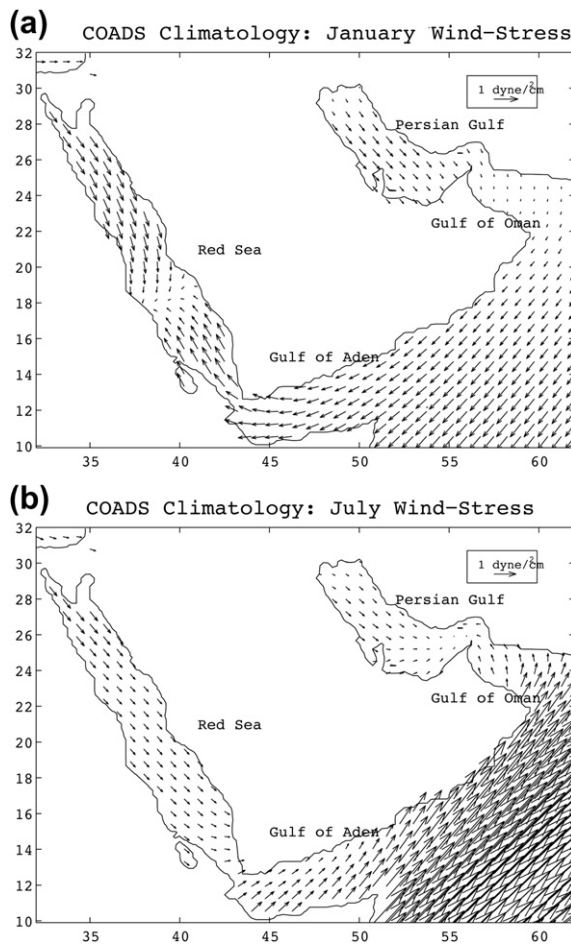

FIGURE S8.26 Wind stress (dyn/cm^2) for the Red Sea and Persian Gulf: (a) January (Northeast Monsoon) and (b) July (Southwest Monsoon). *Sources: From Johns et al. (1999); see also Sofianos and Johns (2003).*

salinity value is not directly comparable to ocean water salinities because the chemical constitution of these brines is quite different. They have a much higher content of metal ions. (For comparison, a saturated solution of sodium chloride in water has a salinity value in the oceanographic sense of about 270.) The favored explanation for the origin of the chemical constituents is that this is interstitial water from sediments or solutions in water of crystallization from solid materials in the sea bottom, which are released by heating from below and forced out through cracks into the deep basins of the Red Sea.

Circulation and formation of hypersaline water in winter in the Persian Gulf was briefly summarized in Section 11.6, based on Johns et al. (2003) and Swift and Bower (2003). The cyclonic circulation, exchange through the Straits of Hormuz, and formation region in the south of the high salinity water mass are illustrated in Figure S8.25b. Winter surface salinity in the southern region exceeds 42 psu. Because the Persian Gulf is so shallow, bottom salinity largely mirrors surface salinity. Inflows of fresher waters from the Gulf of Oman in the southeast and from the Tigris and Euphrates rivers in the northwest bracket the high salinity region along the coast of the Arabian Peninsula. Outflow of the dense water occurs throughout the year, with only a weak seasonal signal, at a mean salinity of 39.5 psu (Johns et al., 2003). Part of the outflow occurs in the surface layer in the southern part of the Straits of Hormuz. The surface layer transport has a strong seasonal cycle.

References

Armi, L., Farmer, D.M., 1988. The flow of Mediterranean Water through the Strait of Gibraltar. Progr. Oceanogr. 21, 1–105 (Also Farmer and Armi, 1988.).

Beardsley, R.C., Boicourt, W.C., 1981. On estuarine and continental-shelf circulation in the Middle Atlantic Bight. In: Warren, B.A., Wunsch, C. (Eds.), Evolution of Physical Oceanography. MIT Press, Cambridge, MA, pp. 198–223.

Bray, N., Ochoa, J., Kinder, T., 1995. The role of the interface in exchange through the Strait of Gibraltar. J. Geophys. Res. 100, 10755–10776.

Bryden, H.L., Candela, J., Kinder, T.H., 1994. Exchange through the Strait of Gibraltar. Progr. Oceanogr. 33, 201–248.

Cameron, W.M., Pritchard, D.W., 1963. Estuaries. In: Hill, M.N. (Ed.), Ideas and Observations. The Sea, Vol. 2. Wiley-Interscience, pp. 306–324.

CIESM, 2001. CIESM Round table session on Mediterranean water mass acronyms. 36th CIESM Congress, Monte Carlo, 26 September 2001. https://www.ciesm.org/catalog/WaterMassAcronyms.pdf (accessed 6.5.09).

Curray, J.R., Emmel, F.J., Moore, D.G., 2003. The Bengal Fan: Morphology, geometry, stratigraphy, history and processes. Mar. Petrol. Geol. 19, 1191–1223.

Dai, A., Trenberth, K.E., 2002. Estimates of freshwater discharge from continents: Latitudinal and seasonal variations. J. Hydromet. 3, 660–687.

Dyer, K.R., 1997. Estuaries: A Physical Introduction, second ed. Wiley, New York, p. 195.

Farmer, D.M., Freeland, H.J., 1983. The physical oceanography of fjords. Progr. Oceanogr. 12, 147–219.

Giosan, L., Filip, F., Constantinescu, S., 2009. Was the Black Sea catastrophically flooded in the early Holocene? Quaternary Sci. Rev. 28, 1–6.

Gladyshev, S., Talley, L., Kantakov, G., Khen, G., Wakatsuchi, M., 2003. Distribution, formation and seasonal variability of Okhotsk Sea Intermediate Water. J. Geophys. Res. 108 (C6), 3186. doi:10.1029/2001JC000877.

Hardisty, J., 2007. Estuaries: Monitoring and Modeling the Physical System. Blackwell Publishing, Maiden, MA. p. 157.

Hu, J., Kawamura, H., Hong, H., Qi, Y., 2000. A review on the currents in the South China Sea: Seasonal circulation, South China Sea Warm Current and Kuroshio intrusion. J. Oceanogr. 56, 607–624.

Jakobsen, F., 1995. The major inflow to the Baltic Sea during January 1993. J. Marine Syst. 6, 227–240.

Johns, W.E., Jacobs, G.A., Kindle, J.C., Murray, S.P., Carron, M., 1999. Arabian Marginal Seas and Gulfs: Report of a Workshop held at Stennis Space Center, Miss. 11–13 May, 1999. University of Miami RSMAS. Technical Report 2000–01.

Karbe, L., 1987. Hot brines and the deep sea environment. In: Edwards, A.J., Head, S.M. (Eds.), Red Sea. Pergamon Press, Oxford, p. 441.

Kelley, D.E., Fernando, H.J.S., Gargett, A.E., Tanny, J., Özsoy, E., 2003. The diffusive regime of double-diffusive convection. Progr. Oceanogr. 56, 461–481.

Kinder, T.H., Coachman, L.K., Galt, J.A., 1975. The Bering Slope Current System. J. Phys. Oceanogr. 5, 231–244.

Klein, B., Roether, W., Civitarese, G., Gacic, M., Manca, B.B., d'Alcalá, M.R., 2000. Is the Adriatic returning to dominate the production of Eastern Mediterranean Deep Water? Geophys. Res. Lett. 27, 3377–3380.

Klein, B., Roether, W., Manca, B.B., Bregant, D., Beitzel, V., Kovacevic, V., Luchetta, A., 1999. The large deep water transient in the Eastern Mediterranean. Deep-Sea Res. I 46, 371–414.

Leppäranta, M., Myrberg, K., 2009. Physical Oceanography of the Baltic Sea. Springer, Berlin, p. 378 with online version.

Malanotte-Rizzoli, P., Manca, B.B., Salvatore Marullo, Ribera d' Alcalá, M., Roether, W., Theocharis, A., Bergamasco, A., Budillon, G., Sansone, E., Civitarese, F. Conversano, F., Gertman, I., Hernt, B., Kress, N., Kioroglou, S., Kontoyannis, H., Nittis, K., Klein, B., Lascaratos, A., Latif, M.A., Özsoy, E., Robinson, A.R., Santoleri, R., Viezzoli, D., Kovacevic, V., 2003. The Levantine Intermediate Water Experiment (LIWEX) Group: Levantine basin — A laboratory for multiple water mass formation processes. J. Geophys. Res. 108(C9), 8101. doi:10.1029/2002JC001643.

Marshall, J., Schott, F., 1999. Open-ocean convection: observations, theory, and models. Rev. Geophys. 37, 1–64.

MEDOC Group, 1970. Observations of formation of deep-water in the Mediterranean Sea, 1969. Nature 227, 1037–1040.

Millot, C., 1991. Mesoscale and seasonal variabilities of the circulation in the western Mediterranean. Dynam. Atmos. Oceans 15, 179–214.

Millot, C., Taupier-Letage, I., 2005. Circulation in the Mediterranean Sea. In: Saliot, E.A. (Ed.), The Handbook of Environmental Chemistry, Vol. 5. Part K. Springer-Verlag, Berlin Heidelberg, pp. 29–66.

Monismith, S.G., 2007. Hydrodynamics of coral reefs. Annu. Rev. Fluid Mech. 39, 37–55.

Murray, J.W., Jannasch, H.W., Honjo, S., Anderson, R.F., Reeburgh, W.S., Top, Z., Friedrich, G.E., Codispoti, L.A., Izdar, E., 1989. Unexpected changes in the oxic/anoxic interface in the Black Sea. Nature 338, 411–413.

Naimie, C.E., Blain, C.A., Lynch, D.R., 2001. Seasonal mean circulation in the Yellow Sea — A model-generated climatology. Continental Shelf Res. 21, 667–695.

NASA Goddard Earth Sciences, 2007c. Sedimentia. NASA Goddard Earth Sciences Ocean Color. http://disc.gsfc.nasa.gov/oceancolor/scifocus/oceanColor/sedimentia.shtml (accessed 4.3.09).

NASA Goddard Earth Sciences, 2008. Ocean color: classic CZCS scenes, Chapter 4. NASA Goddard Earth Sciences Data Information Services Center. http://disc.gsfc.nasa.gov/oceancolor/scifocus/classic_scenes/04_classics_arabian.shtml (accessed 1.9.09).

Neilson, B.J., Kuo, A., Brubaker, J., 1989. Estuarine Circulation. Humana Press, Clifton, N.J., p. 377.

Noaa Ngdc, 2008. Global Relief Data — ETOPO. NOAA National Geophysical Data Center. http://www.ngdc.noaa.gov/mgg/global/global.html (accessed 9.24.08).

Officer, C.B., 1976. Physical Oceanography of Estuaries (and Associated Coastal Waters). Wiley, New York, p. 465.

Oguz, T., Tugrul, S., Kideys, A.E., Ediger, V., Kubilay, N., 2006. Physical and biogeochemical characteristics of the Black Sea. In: Robinson, A.R., Brink, K.H. (Eds.), The Sea. The Global Coastal Ocean: Interdisciplinary Regional Studies and Syntheses, Vol., 14A. Harvard University Press, pp. 1333–1372.

Özsoy, E., Hecht, A., Ünlüata, Ü., Brenner, S., Oguz, T., Bishop, J., Latif, M.A., Rozentraub, Z., 1991. A review of the Levantine Basin circulation and its variability during 1985–1988. Dynam. Atmos. Oceans 15, 421–456.

Özsoy, E., Ünlüata, U., 1998. The Black Sea. In: Robinson, A.R., Brink, K.H. (Eds.), The Sea. The Global Coastal Ocean: Regional Studies and Syntheses, Vol. 11. Harvard University Press, pp. 889–914.

Pickard, G.L., 1961. Oceanographic features of inlets in the British Columbia mainland coast. J. Fish. Res. Bd. Can. 18, 907–999.

Pickard, G.L., Donguy, J.R., Hénin, C., Rougerie, F., 1977. A review of the physical oceanography of the Great Barrier Reef and western Coral Sea. Australian Institute of Marine Science, 2. Australian Government Publishing Service, p. 134.

Pickard, G.L., Stanton, B.R., 1980. Pacific fjords — A review of their water characteristics, pp. 1–51. In: Freeland, H.J., Farmer, D.M., Levings, C.D. (Eds.), Fjord Oceanography. Plenum Press.

Potter, R.A., Lozier, M.S., 2004. On the warming and salinification of the Mediterranean outflow waters in the North Atlantic. Geophys. Res. Lett. 31, L01202. doi:10.1029/2003GL018161.

Price, J.F., Baringer, M.O., 1994. Outflows and deep water production by marginal seas. Progr. Oceanogr. 33, 161–200.

Pritchard, D.W., 1989. Estuarine classification — A help or a hindrance. In: Neilson, B.J., Kuo, A., Brubaker, J. (Eds.), Estuarine Circulation. Humana Press, Clifton, N.J, pp. 1–38.

Reed, R.K., 1995. On geostrophic reference levels in the Bering Sea basin. J. Oceanogr. 51, 489–498.

Roach, A.T., Aagaard, K., Pease, C.H., Salo, S.A., Weingartner, T., Pavlov, V., Kulakov, M., 1995. Direct measurements of transport and water properties through the Bering Strait. J. Geophys. Res. 100, 18443–18458.

Robinson, A.R., Golnaraghi, M., Leslie, W.G., Artegiani, A., Hecht, A., Lazzoni, E., Michelato, A., Sansone, E., Theocharis, A., Ünlüata, Ü, 1991. The eastern

Mediterranean general circulation: features, structure and variability. Dynam. Atmos. Oceans 15, 215−240.

Rodhe, J., 1998. The Baltic and North Seas: A process-oriented review of the physical oceanography. In: Robinson, A.R., Brink, K.H. (Eds.), The Sea. The Global Coastal Ocean: Regional Studies and Syntheses, Vol. 11. Harvard University Press, pp. 699−732.

Rodhe, J., Tett, P., Wulff, F., 2006. The Baltic and North Seas: A regional review of some important physical-chemical-biological interaction processes. In: Robinson, A.R., Brink, K.H. (Eds.), The Sea. The Global Coastal Ocean: Interdisciplinary Regional Studies and Syntheses, Vol., 14A. Harvard University Press, pp. 1033−1076.

Ross, D.A., 1983. The Red Sea. In: Ketchum, B.H. (Ed.), Estuaries and Enclosed Seas. Ecosystems of the World, 26. Elsevier, pp. 293−307.

Rougerie, F., 1986. Le lagon sud-ouest de Nouvelle-Calédonie: spécificité hydrologique, dynamique et productivité. Etudes et Thèses. ORSTOM, Paris, p. 234.

Sankey, T., 1973. The formation of deep water in the North-western Mediterranean. Progr. Oceanogr. 6, 159−179.

Schlitzer, R., Roether, W., Oster, H., Junghans, H.-G., Hausmann, M., Johannsen, H., Michelato, A., 1991. Chlorofluoromethane and oxygen in the Eastern Mediterranean. Deep-Sea Res. 38, 1531−1551.

Sofianos, S.S., Johns, W.E., 2003. An Oceanic General Circulation Model (OGCM) investigation of the Red Sea circulation: 2. Three-dimensional circulation in the Red Sea. J. Geoph. Res. 108, 3066. doi: 10, 1029/200IJC001185.

Stabeno, P.J., Reed, R.K., 1995. Circulation in the Bering Sea basin observed by satellite-tracked drifters: 1986−1993. J. Phys. Oceanogr. 24, 848−854.

Swift, S.A., Bower, A.S., 2003. Formation and circulation of dense water in the Persian/Arabian Gulf. J. Geophys. Res. 108 (C10). doi:10.1029/2002JC001360.

Talley, L.D., 2008. Freshwater transport estimates and the global overturning circulation: Shallow, deep and throughflow components. Progr. Oceanogr. 78, 257−303. doi:10.1016/j.pocean.2008.05.001.

Talley, L.D., Min, D.-H., Lobanov, V.B., Luchin, V.A., Ponomarev, V.I., Salyuk, A.N., Shcherbina, A.Y., Tishchenko, P.Y., Zhabin, I., 2006. Japan/East Sea water masses and their relation to the sea's circulation. Oceanography 19, 33−49.

Teague, W.J., Ko, D.S., Jacobs, G.A., Perkins, H.T., Book, J.W., Smith, S.R., Chang, K.-I., Suk, M.-S., Kim, K., Lyu, S.J., Tang, T.Y., 2006. Currents through the Korea/Tsushima Strait. Oceanography 19, 50−63.

Timmermans, M.L., Garrett, C., Carmack, E., 2003. The thermohaline structure and evolution of the deep waters in the Canada Basin, Arctic Ocean. Deep-Sea Res. I 50, 1305−1321.

Tomczak, M., Godfrey, J.S., 1994. Regional Oceanography, an Introduction. Pergamon Press, Oxford, UK, p. 422.

Tully, J.P., 1949. Oceanography and prediction of pulp-mill pollution in Alberni Inlet. Fish. Res. Bd. Can. Bull. 83, 169.

Wijffels, S.E., Schmitt, R.W., Bryden, H.L., Stigebrandt, A., 1992. Transport of fresh water by the oceans. J. Phys. Oceanogr. 22, 155−162.

Winsor, P., Rodhe, J., Omstedt, A., 2001. Baltic Sea ocean climate: An analysis of 100 yr of hydrographic data with focus on freshwater budget. Climate Res. 18, 5−15.

Winther, N.G., Johannessen, J.A., 2006. North Sea circulation: Atlantic inflow and its destination. J. Geophys. Res. 111 C12018. doi:10.1029/2005JC003310.

Wolanski, E. (Ed.), 2001. Oceanographic Processes of Coral Reefs: Physical and Biological Links in the Great Barrier Reef. CRC Press, Boca Raton, FL, p. 356.

Woodgate, R.A., Aagaard, K., 2005. Revising the Bering Strait freshwater flux into the Arctic Ocean. Geophys. Res. Lett. 32 L02602. doi:10.1029/2004GL021747.

Wüst, G., 1961. On the vertical circulation of the Mediterranean Sea. J. Geophys. Res. 66, 3261−3271.

Xue, H., Chai, F., Pettigrew, N., Xu, D., Shi, M., Xu, J., 2004. Kuroshio intrusion and the circulation in the South China Sea. J. Geophys. Res. 109 C02017. doi:10.1029/2002JC001724.